

OPEN

SUBJECT AREAS:  
HEPATITIS C VIRUS  
DRUG REGULATION

Received  
3 February 2014

Accepted  
27 March 2014

Published  
15 April 2014

Correspondence and  
requests for materials  
should be addressed to  
M.H. (mhonda@  
kanazawa.jp) or S.K.  
(skaneko@  
kanazawa.jp)

# The Acyclic Retinoid Peretinoin Inhibits Hepatitis C Virus Replication and Infectious Virus Release *in Vitro*

Tetsuro Shimakami<sup>1</sup>, Masao Honda<sup>1</sup>, Takayoshi Shirasaki<sup>1</sup>, Riuta Takabatake<sup>1</sup>, Fanwei Liu<sup>1</sup>, Kazuhisa Murai<sup>1</sup>, Takayuki Shiimoto<sup>1</sup>, Masaya Funaki<sup>1</sup>, Daisuke Yamane<sup>2</sup>, Seishi Murakami<sup>1</sup>, Stanley M. Lemon<sup>2</sup> & Shuichi Kaneko<sup>1</sup>

<sup>1</sup>Department of Gastroenterology, Kanazawa University Hospital, Kanazawa, Ishikawa 920-8641, Japan, <sup>2</sup>Lineberger Comprehensive Cancer Center and the Division of Infectious Diseases, Department of Medicine, The University of North Carolina at Chapel Hill, Chapel Hill, NC 27599-7292, USA.

Clinical studies suggest that the oral acyclic retinoid Peretinoin may reduce the recurrence of hepatocellular carcinoma (HCC) following surgical ablation of primary tumours. Since hepatitis C virus (HCV) infection is a major cause of HCC, we assessed whether Peretinoin and other retinoids have any effect on HCV infection. For this purpose, we measured the effects of several retinoids on the replication of genotype 1a, 1b, and 2a HCV *in vitro*. Peretinoin inhibited RNA replication for all genotypes and showed the strongest antiviral effect among the retinoids tested. Furthermore, it reduced infectious virus release by 80–90% without affecting virus assembly. These effects could be due to reduced signalling from lipid droplets, triglyceride abundance, and the expression of mature sterol regulatory element-binding protein 1c and fatty acid synthase. These negative effects of Peretinoin on HCV infection may be beneficial in addition to its potential for HCC chemoprevention in HCV-infected patients.

Hepatitis C virus (HCV) is a causative agent of chronic hepatitis, liver cirrhosis, and hepatocellular carcinoma (HCC); therefore, the eradication of HCV from an infected liver could reduce death from HCV-related liver disease. Combination therapy of PEGylated-interferon (PEG-IFN) and ribavirin has long been the standard of care for patients with chronic hepatitis C (CH-C); however, a sustained viral response (SVR) is obtained in only ~50% of treated patients infected with genotype 1 HCV<sup>1</sup>. Recently, several classes of direct-acting antiviral agents (DAAs) have entered into clinical use. In the United States, two NS3/4A protease inhibitors, telaprevir and boceprevir, were approved for use in combination with PEG-IFN and ribavirin in 2011. Although the addition of these DAAs dramatically improves the SVR rate, 20–30% of patients still fail to eradicate HCV due to breakthrough by drug-resistant mutants or null response to therapy<sup>2</sup>. More potent DAAs are currently in late clinical development and promise much higher SVR rates even in the absence of PEG-IFN therapy; however, HCV-related HCC is likely to continue to be a significant clinical issue for many years because it will take time for potent DAAs to be distributed worldwide.

Peretinoin (generic name code: NIK-333) is an oral acyclic retinoid with a vitamin A-like structure that targets retinoid nuclear receptors, such as retinoid X receptor and retinoic acid receptor. The oral administration of Peretinoin significantly reduces the incidence of post-therapeutic HCC recurrence and improves the survival rate of patients in clinical trials<sup>3,4</sup>. In addition, Peretinoin prevents the development of hepatoma in several different hepatoma models<sup>5,6</sup>. Larger-scale clinical studies are currently ongoing in various countries to confirm its clinical efficiency. Depending on the results of these studies, Peretinoin may be used in CH-C patients to prevent HCC. Therefore, we sought to understand the effect of Peretinoin on HCV replication.

Peretinoin is categorised as a vitamin A or retinoid compound, and conflicting reports have described the effects of vitamin A compounds on HCV replication. One report showed that 3 retinoids, 9-*cis* retinoic acid (RA), 13-*cis* RA, and all-*trans* RA (ATRA), suppressed the replication of a sub-genomic HCV replicon<sup>7</sup>. However, vitamin A also reportedly enhances the replication of genome-length HCV in Huh-7 cells<sup>8</sup>. Here, we describe the impact of Peretinoin on different steps of the HCV life cycle, including translation, RNA amplification, virus assembly, and secretion, and its impact on host lipid metabolism *in vitro*. Our results clearly demonstrate that Peretinoin inhibits HCV RNA amplification and virus release by altering lipid metabolism.



## Results

**Inhibition of HCV RNA replication by retinoids.** Several studies have tested the effects of vitamin A on HCV replication; these studies used a sub-genomic or full-genomic replicon, which contains 2 cistrons, one driven by HCV internal ribosome entry sites (IRES) and the other by encephalomyocarditis virus IRES<sup>7,8</sup>. We reported the usefulness of HCV genomes containing *Gaussia princeps* luciferase (GLuc) between p7 and NS2, followed by foot-and-mouth disease virus 2A, to monitor HCV RNA replication<sup>9,10</sup>, and this system is closer to physiological HCV replication than the bicistronic replicon systems (Fig. 1A). In addition to GLuc-containing HCV genomes in the backbone of genotype 1a H77S.3, a chimeric clone of H77S and genotype 2a JFH1, HJ3-5<sup>11</sup>, with structural proteins from H77S and non-structural proteins from JFH1, we also constructed GLuc-containing genomes in the backbone of genotype 1b N<sup>12</sup> and 2a JFH1<sup>13</sup> and confirmed their efficient replication in Huh-7.5 cells. Importantly, all of the strains used here are derived from cDNA clones that are infectious to chimpanzees.

We initially examined the effects of 4 different retinoids, namely ATRA, 9-cis RA, 13-cis RA, and Peretinoin, on HCV replication by using these 4 HCV genomes containing GLuc, according to the use of GLuc activity as an indicator of RNA replication, and the structures of each retinoid were shown in Supplementary Fig. S1 online. Peretinoin inhibited the replication of H77S.3/GLuc2A in a dose-dependent manner (Fig. 1B). As the other retinoids also suppressed HCV replication, we determined the antiviral half maximal effective concentrations (EC<sub>50</sub>s) of these retinoids for each HCV genotype. Whilst Peretinoin showed the strongest antiviral effect on all genotypes tested, ATRA exerted a moderate effect, and 9-cis and 13-cis RA generated a weaker effect (Table 1). Especially, Peretinoin suppressed the RNA replication of H77S.3/GLuc2A most efficiently and its EC<sub>50</sub> was 9 μM.

We also determined the half maximal cytotoxicity concentrations (CC<sub>50</sub>s) of these retinoids in H77S.3/GLuc2A-replicating Huh-7.5 cells by using the WST-8 assay, which reflects cell number. The CC<sub>50</sub>s of ATRA, 9-cis RA, and 13-cis RA were more than 100 μM; however, the CC<sub>50</sub> of Peretinoin was 68 μM when the cells were treated for 72 h (Table 2). Although Peretinoin had a slightly negative impact on cell growth, as it showed the strongest antiviral effect and may be used for HCC chemoprevention in HCV-infected patients in the future, we focused upon the action of Peretinoin among these retinoids.

**Inhibition of HCV RNA replication by Peretinoin.** We examined the time dependence of the antiviral effect of Peretinoin. After HCV RNA transfection, we treated the transfected cells with Peretinoin at a range of concentrations (10–40 μM) and monitored RNA replication every 24 h until 72 h. Peretinoin started to show an antiviral effect from 24 h after treatment, which continued until 72 h. Peretinoin suppressed RNA replication in a time-dependent manner for all genotypes tested (Fig. 1C).

We also examined whether Peretinoin could also suppress RNA replication in a sub-genomic replicon system (Fig. 1D), in which infection should not occur due to the lack of structural proteins. Peretinoin was also able to suppress RNA replication in a dose-dependent manner in bicistronic sub-genomic RNA-transfected cells (Fig. 1E).

Importantly, when we treated HCV (H77S.3/GLuc2A)-replicating and HCV-non-replicating Huh-7.5 cells with Peretinoin at a range of concentrations (5–50 μM), the cell numbers were identical under the conditions tested (Fig. 1F).

As Peretinoin could suppress GLuc activity itself, we then examined directly its antiviral effect in the context of an HCV genome lacking the GLuc genome. For this purpose, Huh-7.5 cells infected with cell culture-derived HCV (HCVcc) of HJ3-5 were treated with

different concentrations of Peretinoin. When we monitored HCV RNA replication by using quantitative real-time detection-polymerase chain reaction (RTD-PCR) (Fig. 2A) and protein expression by western blotting for the HCV core protein (Fig. 2B, see Supplementary Fig. S2 online), Peretinoin suppressed RNA replication and protein expression in a dose-dependent manner, which is consistent with the GLuc activity results. We also tested infectious virus production from Peretinoin-treated cells using a conventional focus forming unit (FFU) assay, and found that Peretinoin also reduced this in a dose-dependent manner (Fig. 2C).

**Effect of Peretinoin on translation driven by HCV IRES.** We also tested the effect of Peretinoin on translation directed by HCV IRES. For this purpose, we used a mini-genome RNA which has, sequentially, the HCV 5'-untranslated region (UTR), GLuc, and HCV 3'-UTR, and cap-*Cypridina* luciferase (CLuc)-polyA RNA as a control (see Supplementary Fig. S1 online). After we treated Huh-7.5 cells with different concentrations of Peretinoin for 24 h, we co-transfected the cells with these RNAs and measured GLuc and CLuc activity every 3 h from 3 to 12 h. When we normalised GLuc activity to CLuc activity at each time point, we did not observe a significant difference among the cells treated with the different concentrations of Peretinoin (see Supplementary Fig. S3 online), suggesting that Peretinoin does not have an effect on protein expression directed by HCV IRES.

**Effect of Peretinoin on cellular interferon signalling.** We hypothesised that the suppression of RNA replication by Peretinoin could be due to the activation or enhancement of cellular interferon (IFN) signalling. To examine this, we treated HCV (H77S.3/GLuc2A)-non-replicating and HCV-replicating Huh-7.5 cells with either IFNα-2b (10 IU/mL) or Peretinoin (10–40 μM) and monitored the expression of total and phosphorylated signal transducer and activator of transcription 1 (STAT1). Peretinoin did not alter the expression of either total or phosphorylated STAT1 in HCV-non-replicating Huh-7.5 cells or HCV-replicating cells (see Supplementary Fig. S4 online). In addition, Peretinoin did not further enhance the amount of phosphorylated STAT1 activated by IFNα-2b in HCV-non-replicating Huh-7.5 cells or HCV-replicating cells (see Supplementary Fig. S4 online). These data suggest that Peretinoin suppresses RNA replication without either activating or enhancing cellular IFN signalling.

**Impact of Peretinoin on lipid metabolism.** As lipid metabolism has an important role in various aspects of HCV infection<sup>14–16</sup>, we examined the impact of Peretinoin on lipid metabolism. However, as it is sometimes difficult to detect small changes in lipid metabolism, we tested the effect of Peretinoin under oleic acid (OA) treatment, which amplifies changes in lipid metabolism. We treated H77S.3/GLuc2A-replicating Huh-7.5 cells with 40 μM Peretinoin and 250 μM OA, fixed and stained the cells with BODIPY 493/503 for lipid droplets (LDs) and 4', 6-diamidino-2-phenylindole (DAPI) for nuclei, and used an anti-core protein antibody to detect HCV. When we stained LDs in the presence of 250 μM OA and the absence of Peretinoin, we observed intense signals (Fig. 3A); however, when it was accompanied with 40 μM Peretinoin, the signals from LDs were dramatically reduced, and at the same time, the expression of HCV core protein was also down-regulated (Fig. 3B). When we quantitated the signal strength from LDs and HCV core protein in 4 different fields, Peretinoin significantly reduced the signals from LDs and HCV core protein (two-tailed Student's t test, p<0.0001 for each) (Fig. 3C). This reduction was also confirmed by the quantitation of the 5 cells which were positive for both LDs and HCV core (see Supplementary Fig. S5 online). The reduced expression of HCV core protein was also observed by western blot analysis (Fig. 3D, see Supplementary Fig. S6 online). We next investigated the

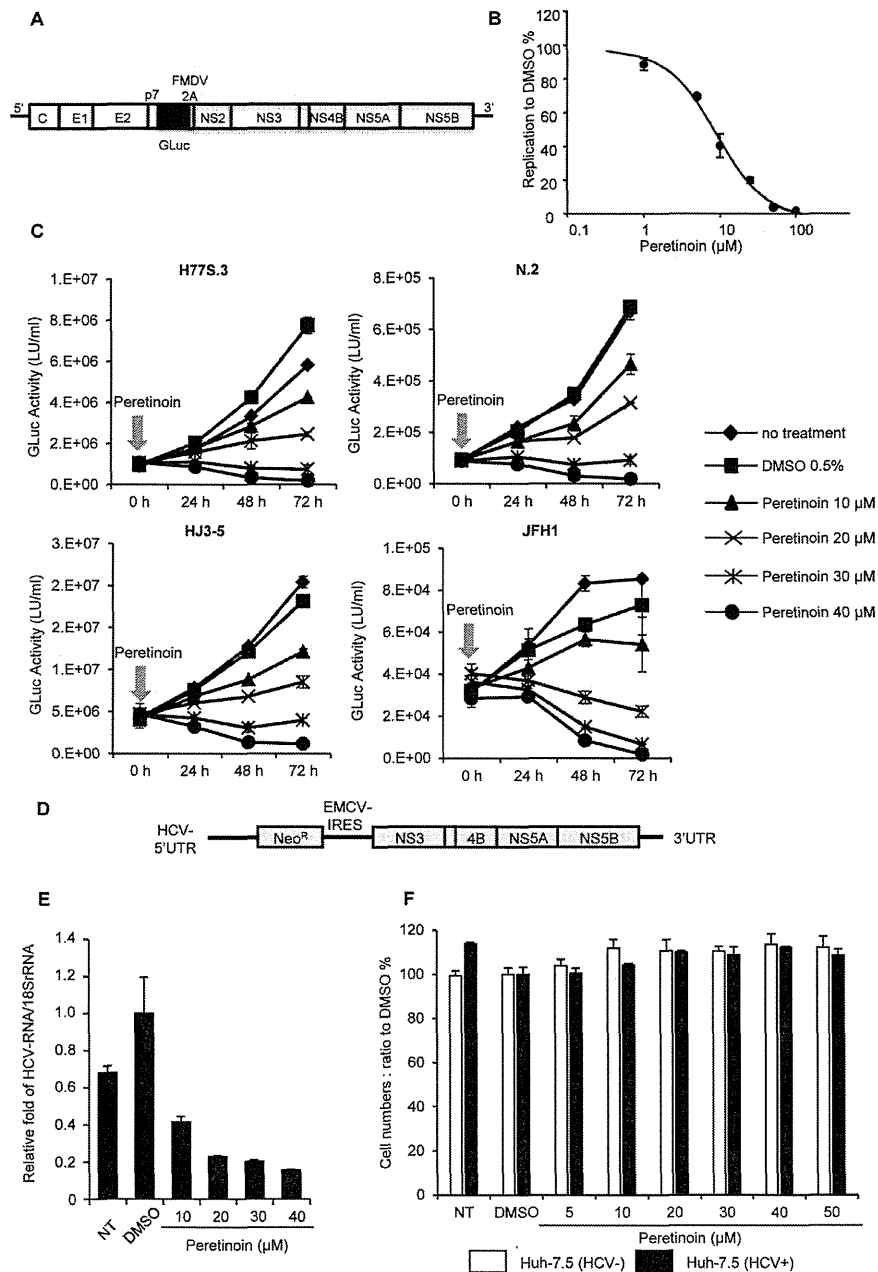


**Figure 1 | Antiviral effects of several retinoids and their effects on cell growth.** (A) Schematic representation of the GLuc-containing HCV genome. (B) Huh-7.5 cells were transfected with H77S.3/GLuc2A RNA, and 48 h later, 0.5% DMSO or Peretinoin was added at concentrations ranging from 1 to 100  $\mu\text{M}$ . Fresh medium containing Peretinoin was added every 24 h, and 72 h after adding Peretinoin, secreted GLuc activity was measured. The GLuc activity from Peretinoin-treated cells was normalised to that with DMSO treatment. Data show the mean inhibition to DMSO treatment in each concentration of Peretinoin  $\pm$  SD from 3 independent experiments. (C) Huh-7.5 cells were transfected with H77S.3/GLuc2A, N.2/GLuc2A, HJ3-5/GLuc2A, and JFH1/GLuc2A RNAs, and 48 h later, 0.5% DMSO or Peretinoin was added at the indicated concentrations. The medium was collected and replaced with fresh medium every 24 h until 72 h. GLuc activity was determined at each time point. The results shown represent the mean GLuc activity  $\pm$  SD from 3 different plates. (D) Schematic representation of the bicistronic sub-genomic HCV RNA (E) Huh-7.5 cells were transfected with bicistronic sub-genomic RNA. At 48 h later, the transfected cells were treated with the indicated concentrations of Peretinoin for 72 h. Quantification of HCV RNA and 18S rRNA levels was performed and relative HCV RNA abundance normalised to the amount of 18S rRNA is presented as fold change  $\pm$  SD compared to DMSO-treated cells from 3 independent experiments. (F) Huh-7.5 cells were transfected with H77S.3/GLuc2A RNA, and 7 days later, HCV (H77S.3/GLuc2A)-replicating Huh-7.5 cells, depicted as 'HCV+', were treated with the indicated concentrations of Peretinoin and HCV-non-replicating Huh-7.5 cells, depicted as 'HCV-', were also treated in a same way. At 72 h after Peretinoin treatment, cell numbers were determined by using a Cell Counting Kit-8. Data represent relative cell numbers  $\pm$  SD from 3 independent experiments to DMSO-treated cells. EMCV, Encephalomyocarditis virus; Neo<sup>R</sup>, Neomycin resistance gene; NT, no treatment.



**Table 1 | EC<sub>50</sub> of vitamin A compounds on HCV RNA replication**

	Peretinoin		ATRA		9-cis RA		13-cis RA	
	Mean	SD	Mean	SD	Mean	SD	Mean	SD
HCV	( $\mu$ M)	( $\mu$ M)	( $\mu$ M)	( $\mu$ M)	( $\mu$ M)	( $\mu$ M)	( $\mu$ M)	( $\mu$ M)
H77S.3	9	1	32	3	29	7	41	4
N.2	19	1	53	5	75	8	83	17
HJ3-5	18	2	25	1	51	6	82	17
JFH1	20	1	25	1	61	8	78	11

impact of Peretinoin on lipid metabolism by measuring intracellular triglyceride (TG) levels, which should mainly reflect the amount of LDs, following treatment with 0–40  $\mu$ M Peretinoin with or without HCV replication and OA treatment. Peretinoin reduced intracellular TG levels in a dose-dependent manner, regardless of OA treatment and HCV replication (Fig. 4A). These effects may be primarily due to its transcriptional modulation. To address this possibility, we examined the effect of Peretinoin on the transcription of fatty acid synthase (FASN) using RTD-PCR under 0–40  $\mu$ M Peretinoin with or without HCV replication and OA treatment, because FASN is a key enzyme for the synthesis of fatty acids, which are an essential component of TGs. Peretinoin reduced the mRNA levels of FASN in a dose-dependent manner, regardless of OA treatment and HCV replication (Fig. 4B). We also examined FASN protein expression as well as the levels of precursor and mature sterol regulatory element-binding protein 1c (SREBP1c), which is a critical transcription factor for FASN. Peretinoin reduced the expression of FASN protein, which is consistent with the RTD-PCR results (Fig. 4C, see Supplementary Fig. S7 online). Although Peretinoin did not have an effect on precursor SREBP1c protein expression, it dramatically reduced the levels of mature SREBP1c (Fig. 4C, see Supplementary Fig. S7 online). We also observed a reduction of FASN mRNA levels by Peretinoin in an immortalised human hepatocyte cell line (Fig. 5A), and a similar reduction was also observed for ATRA, 9-cis RA, and 13-cis RA treatment of HCV-replicating Huh-7.5 cells (Fig. 5B). These results indicate that Peretinoin reduced intracellular lipid levels by reducing the amount of mature SREBP1c and, subsequently, FASN.

**Specific inhibition of virus secretion by Peretinoin.** Recently, lipids including LDs and TG have been reported to be important for efficient infectious virus production<sup>14–16</sup>. Due to its huge impact on lipid metabolism, Peretinoin could affect virus assembly or secretion as well as RNA amplification. To test the effect of Peretinoin on infectious virus production, we determined intra- and extra-cellular infectivity and the virus secretion ratio by measuring the amount of intra- and extra-cellular infectious virus from HJ3-5/GLuc2A-replicating FT3-7 cells treated with various concentrations of Peretinoin. We infected naïve Huh-7.5 cells with intra- and extra-cellular virus derived from HJ3-5/GLuc2A-replicating cells after Peretinoin treatment and used GLuc activity as an indicator of infectious virus production because FFUs and GLuc activity were well correlated (see Supplementary Fig. S8 online),

**Table 2 | CC<sub>50</sub> of vitamin A compounds on Huh-7.5 cells supporting HCV replication**

Peretinoin		ATRA	9-cis RA	13-cis RA
Mean	SD	Mean	Mean	Mean
( $\mu$ M)	( $\mu$ M)	( $\mu$ M)	( $\mu$ M)	( $\mu$ M)
68	5.2	>100	>100	>100

and a previous report also showed a good correlation between them<sup>17</sup>. Although Peretinoin did not show a significant impact on intracellular infectivity at 10–30  $\mu$ M, it dramatically reduced extracellular infectivity and virus secretion from 10  $\mu$ M when we normalised intra- and extra-cellular infectivity by the replication capacity of the virus producing the intra- and extra-cellular virus, as determined by GLuc activity (Fig. 6A). This result was also confirmed by using the extra-cellular virus which was prepared by centrifugation and subsequently re-suspended to fresh medium without containing Peretinoin, indicating that possible carryover of Peretinoin in the medium from extra-cellular cultures does not affect the result shown in Figure 6A (Supplementary Fig. S9 online). Interestingly, the expression of apolipoprotein E3 (ApoE3), which is essential for virus secretion, was also suppressed by Peretinoin (Fig. 4C, see Supplementary Fig. S7 online). Furthermore, we compared the buoyant density of HCVcc derived from HJ3-5/GLuc2A-replicating FT3-7 cells by equilibrium gradient ultracentrifugation. HCVcc from HJ3-5/GLuc2A-replicating cells treated with dimethyl sulfoxide (DMSO) or 30  $\mu$ M Peretinoin showed exactly the same peak of infectivity at 1.107 g/cm<sup>3</sup> (Fig. 6B, 6C). Specific infectivity, as calculated from both peaks of HCV RNA and GLuc activity, was  $0.0381 \pm 0.0209$  (standard deviation, SD) light units (LU)/copy for DMSO-treated cells, and  $0.0799 \pm 0.0457$  LU/copy for Peretinoin-treated cells, which did not show a considerable difference. Furthermore, Peretinoin did not affect virus entry of HCVcc when we tested it by RT-PCR for HCV RNA at 5 h after infection and an FFU assay at 72 h after infection (see Supplementary Fig. S10 online). Collectively, Peretinoin seems to inhibit virus release in addition to viral RNA amplification.

## Discussion

In the present study, we clearly showed that Peretinoin, as well as ATRA, 9-cis RA, and 13-cis RA, suppressed HCV RNA replication (Table 1). While previous reports used replicon systems to test the effects of retinoids, we used a genome-length HCV containing a GLuc-coding sequence between p7 and NS2, which is more physiological than replicons. The inhibitory effect of retinoids was universal among the HCV genotypes tested, and all retinoids tested showed an inhibitory effect on HCV replication (Table 1). In addition, we also observed the antiviral effect of Peretinoin in the replicon system (Fig. 1E). Therefore, our present data strongly support the notion that retinoids exert an antiviral effect *in vitro*. The antiviral effect of retinoids has also been confirmed in a clinical study. Even when CH-C patients were treated with ATRA, the viral load dropped by 1–2 log units in 50% of the patients enrolled. In addition, when CH-C patients who showed no response to prior IFN/PEG-IFN $\alpha$  and ribavirin therapy were treated with a combination of ATRA and PEG-IFN $\alpha$ -2a, 30% of patients showed a significant viral reduction<sup>18</sup>. Recently, combined vitamin A and D deficiency prior to IFN-based therapy was shown to be a strong independent predictor of non-response to antiviral therapy<sup>19</sup>. Collectively, our data and the clinical findings indicate that retinoids possess inhibitory effects on HCV replication.

Peretinoin showed the strongest antiviral effect among the retinoids tested (Table 1); thus, we focused on Peretinoin to clarify its antiviral mechanism. A previous report showed that 9-cis RA enhanced the antiviral effect of IFN $\alpha$  by increasing the expression of the IFN $\alpha$  receptor<sup>20</sup>; however, another study showed that ATRA did not induce the activation of dsRNA-activated protein kinase R, which is a key player in the IFN-induced antiviral response<sup>7</sup>. In the present study, Peretinoin did not increase the amount of the activated form of STAT-1, which is pSTAT1, contrary to IFN $\alpha$ -2b, both in HCV-replicating and HCV-non replicating Huh-7.5 cells, and dual treatment of Huh-7.5 cells with IFN $\alpha$ -2b and Peretinoin did not show a further increase of the pSTAT1 levels induced by only IFN $\alpha$ -2b (see Supplementary Fig. S4 online), indicating that

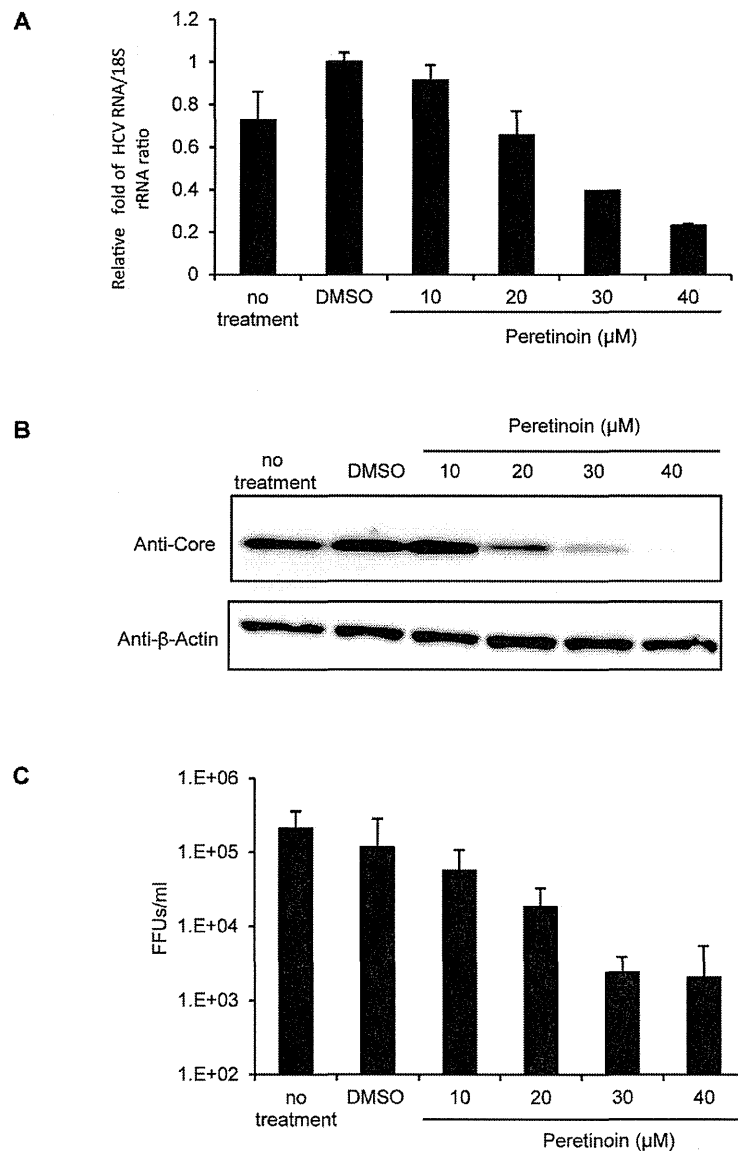


**Figure 2 | Inhibition of HCV replication and infectious virus production.** Huh-7.5 cells were infected with the HJ3-5 virus at a multiplicity of infection (MOI) of 1, and 72 h later, DMSO or Peretinoin was added at the indicated concentrations. The medium was replaced with fresh medium every 24 h until 72 h. (A) At 72 h after adding Peretinoin, total cellular RNA was extracted, and the amount of HCV RNA and 18S rRNA was quantitated by RTD-PCR. Relative HCV RNA abundance normalised to the amount of 18S rRNA is presented as fold change  $\pm$  SD compared to DMSO-treated cells from 3 independent experiments. (B) At 72 h after Peretinoin treatment, the cell lysates were collected and subjected to western blot analysis using anti-core protein and anti- $\beta$ -actin antibodies. Full-length blots/gels are presented in Supplementary Fig. S2 online. (C) The medium was collected at 72 h after Peretinoin treatment, and immediately, naïve Huh-7.5 cells were infected with serially diluted medium. At 72 h after infection, the infectious virus titre of HCVcc from Peretinoin-treated cells was determined by an FFU assay. Data shown here represent the mean FFUs/mL  $\pm$  SD from 2 independent experiments.

Peretinoin did not activate or enhance cellular IFN signalling. Our results also indicate that the antiviral effect of Peretinoin is not due to the suppression of HCV translation directed by HCV IRES (see Supplementary Fig. S3 online). As Peretinoin suppressed the RNA replication of bicistronic sub-genomic replicons (Fig. 1E), it seems to suppress RNA amplification itself (see also the later description of FASN). A report showed that retinoids inhibited HCV RNA replication by enhancing the expression of gastrointestinal-glutathione peroxidase (GI-GPx) only in the presence of sodium selenite<sup>14</sup>; however,

in the present study, we demonstrated that all retinoids tested inhibited HCV replication, even in the absence of sodium selenite. Thus, our results support the notion that the observed antiviral effects could be independent of GI-GPx, although supplementation with sodium selenite may further enhance the antiviral effects of retinoids.

To clarify the mechanism underlying the antiviral effect of Peretinoin further, we focused on the effect of Peretinoin on lipid metabolism because it has been shown to modify multiple aspects of HCV infection<sup>14–16</sup>, and we detected a significant reduction of FASN

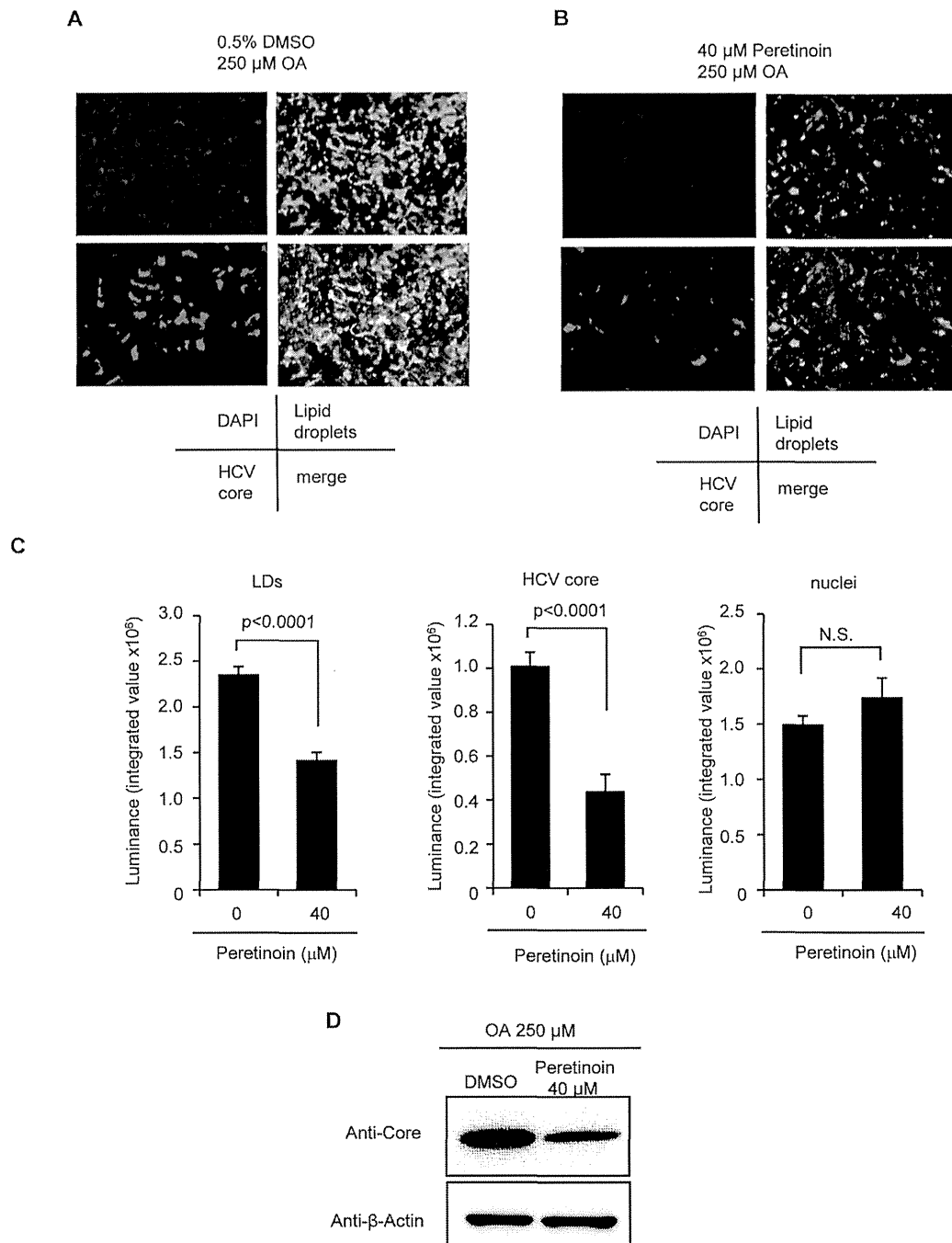


**Figure 3** | Reduction of LD signals by Peritoinoin. Huh-7.5 cells were infected with HJ3-5 virus at an MOI of 1, and 72 h later, 250  $\mu$ M OA and DMSO or 250  $\mu$ M OA and 40  $\mu$ M Peritoinoin were added, and the following assay was performed at 72 h later. (A, B) At 72 h later, the cells were fixed and stained for nuclei, LDs, and HCV core protein. (A) Shows 250  $\mu$ M OA and DMSO-treated cells and (B) shows 250  $\mu$ M OA and 40  $\mu$ M Peritoinoin-treated cells. The photos in (A) and (B) were taken under exactly the same conditions. (C) The signal intensity from LDs, HCV core protein, and nuclei was quantitated as described in the Methods. Data shown represent mean signal intensity  $\pm$  SD from 4 different areas, and the difference was analysed statistically using Student's t-test. (D) Cell lysates were collected and subjected to western blot analysis using anti-core protein and anti- $\beta$ -actin antibodies. Full-length blots/gels are presented in Supplementary Fig. S6 online. N.S., not significant.

mRNA levels by Peritoinoin in a mouse hepatoma model, implying its possible effect on lipid metabolism<sup>5</sup>. Surprisingly, Peritoinoin strongly reduced the signal from LDs in the presence of OA and intracellular TGs (Fig. 3A–C, 4A). LDs are known to have an

essential role in the assembly of HCV virus particles by interacting with HCV core protein and NS5A<sup>21,22</sup>. Therefore, we examined the effect of Peritoinoin on several steps of infectious virus production, such as assembly and secretion. Interestingly, Peritoinoin specifically

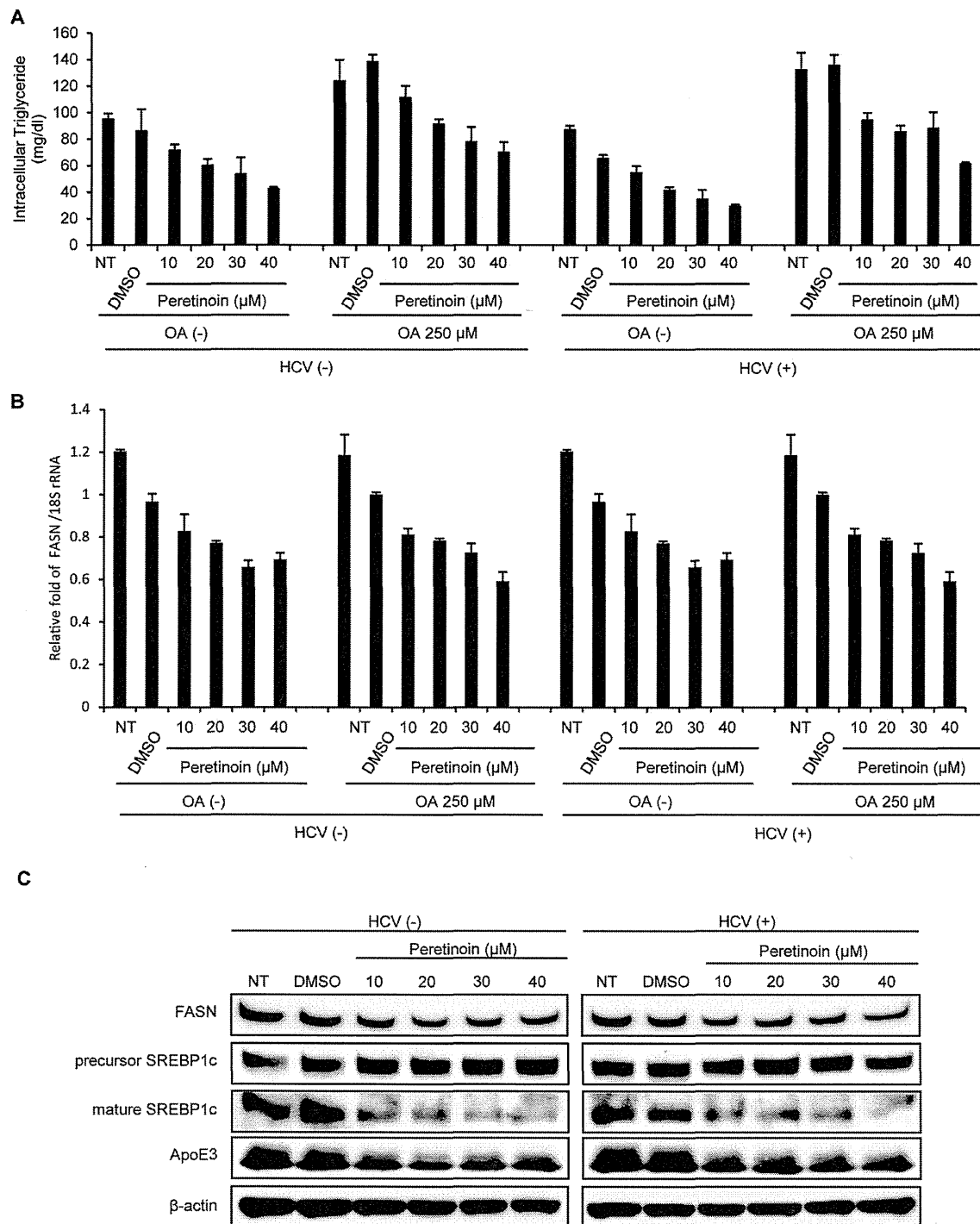


**Figure 4 | Mechanism by which Peretinoin alters lipid metabolism.** Huh-7.5 cells were transfected with H77S.3/GLuc2A RNA, and 72 h later, the transfected cells, depicted as 'HCV(+)', and non-transfected Huh-7.5 cells, depicted as 'HCV(-)', were treated with or without 250 μM OA in the presence of 2% fatty acid-free BSA with 0.5% DMSO or 10–40 μM Peretinoin, and the following assay was performed at 72 h later. (A) The concentration of intracellular TGs was measured. Data shown represent mean concentration ± SD from 3 independent experiments. (B) RNA was extracted and the levels of FASN mRNA and 18S rRNA were quantitated by RTD-PCR. FASN levels were normalised to those of 18S rRNA, and the ratio was furthermore normalised to that from DMSO-treated cells. The results presented here represent the relative fold of FASN/18S rRNA ± SD from 3 independent experiments at the indicated conditions. (C) Lysates from the cells without OA treatment were collected and subjected to western blot analysis using anti-FASN, anti-precursor SREBP1c, anti-mature SREBP1c, anti-ApoE3, and anti-β-actin antibodies. Full-length blots/gels are presented in Supplementary Fig. S7 online.

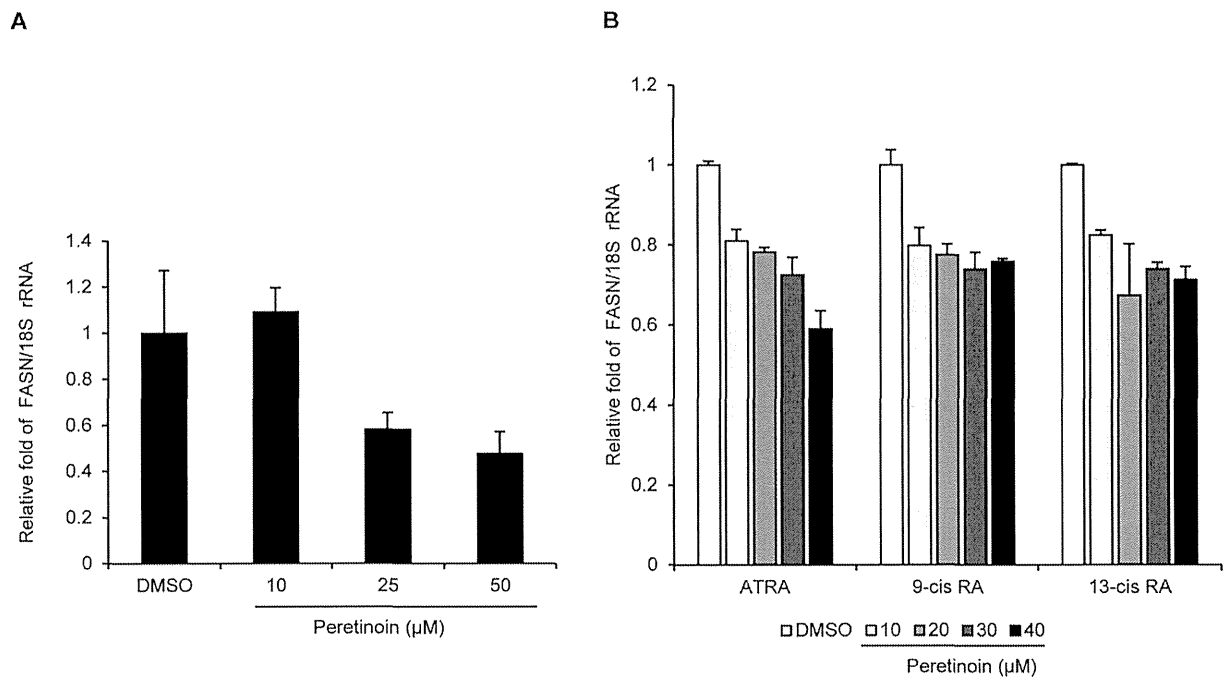


**Figure 5 | Reduction of FASN mRNA levels by Peretinoin in a human hepatocyte cell line and the effects of ATRA, 9-cis RA, and 13-cis RA on the expression of FASN mRNA.** (A) An immortalised human hepatocyte cell line, THLE-5b cells, was treated with the indicated concentrations of Peretinoin. At 72 h later, RNA was extracted and reverse transcribed, and the levels of FASN mRNA and 18S rRNA were quantified by RTD-PCR. The relative amount of FASN mRNA normalised to that of 18S rRNA is presented as fold change compared to DMSO-treated cells from 3 independent experiments at the indicated conditions. (B) Huh-7.5 cells were transfected with H77S.3/GLuc2A RNA. At 72 h later, the transfected cells were treated with DMSO or 10–40 μM ATRA, 9-cis RA, and 13-cis RA. At 72 h later, RNA was extracted and the levels of FASN mRNA and 18S rRNA were quantified by RTD-PCR. The relative amount of FASN mRNA was determined as described in Fig. 4 and presented as fold change compared to DMSO-treated cells from 3 independent experiments at the indicated conditions.

impaired virus secretion without affecting assembly at 10–30 μM, whilst 40 μM Peretinoin impaired virus secretion and assembly (Fig. 6A). The role of LDs in virus secretion has not been fully characterised, but virus should be secreted through the production and release of very low-density lipoproteins. In addition to microsomal triglyceride transfer protein and several apolipoproteins, such as ApoB and ApoE<sup>23</sup>, small interfering RNA screening revealed that multiple components of the secretory pathway, including endoplasmic reticulum to Golgi trafficking and lipid and protein kinases, are involved in HCV secretion<sup>24</sup>. Thus, the mechanism underlying this specific inhibition of virus secretion by Peretinoin remains to be addressed. One possible explanation for its action is the reduction of ApoE3 expression (Fig. 4C), because ApoE3 was shown to have an important role in virus secretion with a minimal impact on assembly<sup>25</sup>.

Several reports showed that LDs play an essential role in RNA amplification and virus assembly. The hypolipidemic agent norethindrone reduced the number of LDs, resulting in the suppression of RNA amplification and virus secretion, as Peretinoin did<sup>26</sup>. Furthermore, inhibition of tail-interacting protein 47, which coats LDs and is involved in their generation and turnover, suppressed HCV RNA replication and assembly<sup>27,28</sup>. Thus, the inhibition of RNA replication by Peretinoin could be explained by its direct effect on LDs. In addition, a recent report suggested that FASN may localise within HCV replication complexes through an interaction with NS5B, thereby increasing its RNA-dependent RNA polymerase activity<sup>29</sup>. Thus, Peretinoin may inhibit RNA replication not only by reducing the signalling of LDs but also inhibiting the expression of FASN.

We also demonstrated that Peretinoin reduced the levels of mature SREBP1c by inhibiting the proteolysis of its precursor, and subsequently the transcription and expression of FASN (Fig. 4C), which could be the main reason for the alteration of lipid metabolism by Peretinoin; however, the mechanism by which it inhibits proteolysis should be addressed in a future study. Several reports have shown that the expression of SREBP1c and/or FASN is increased in HCV-infected patients<sup>30</sup>, Huh-7 cells<sup>31</sup>, and a transgenic mouse expressing the full-length HCV polyprotein<sup>32</sup>. In addition, HCV infection was shown to enhance the proteolytic cleavage of precursor SREBP1c, resulting in an increase in its mature form<sup>33</sup>. Taken together, HCV induces lipogenesis to make infected cells more supportive for its propagation. In contrast to HCV, Peretinoin seems to suppress lipogenesis by inhibiting the SREBP1c-FASN axis, which is highly activated by HCV infection. It is also important to note that this effect did not depend on HCV infection, indicating that Peretinoin should exert a hypolipidemic effect, as we also observed a reduction of FASN mRNA levels following Peretinoin treatment of an immortalised human hepatocyte cell line (Fig. 5A). Interestingly, this effect was universal among retinoids because the other retinoids examined also reduced FASN mRNA levels (Fig. 5B). These findings suggest that Peretinoin could also be useful for the treatment of non-alcoholic fatty liver disease, whose hallmark is hepatic fat accumulation.

The antiviral EC<sub>50</sub> of Peretinoin seems to be closer to its CC<sub>50</sub> than that of the other retinoids in Huh-7.5 cells because several papers have shown that Peretinoin inhibits the growth of hepatoma cells *in vivo* and *in vitro*<sup>34,35</sup>, induces apoptosis in human hepatoma cell lines<sup>36</sup>, and causes an arrest of the cell cycle in G0-G1 in human hepatoma cell lines<sup>35</sup>, indicating that Peretinoin should selectively



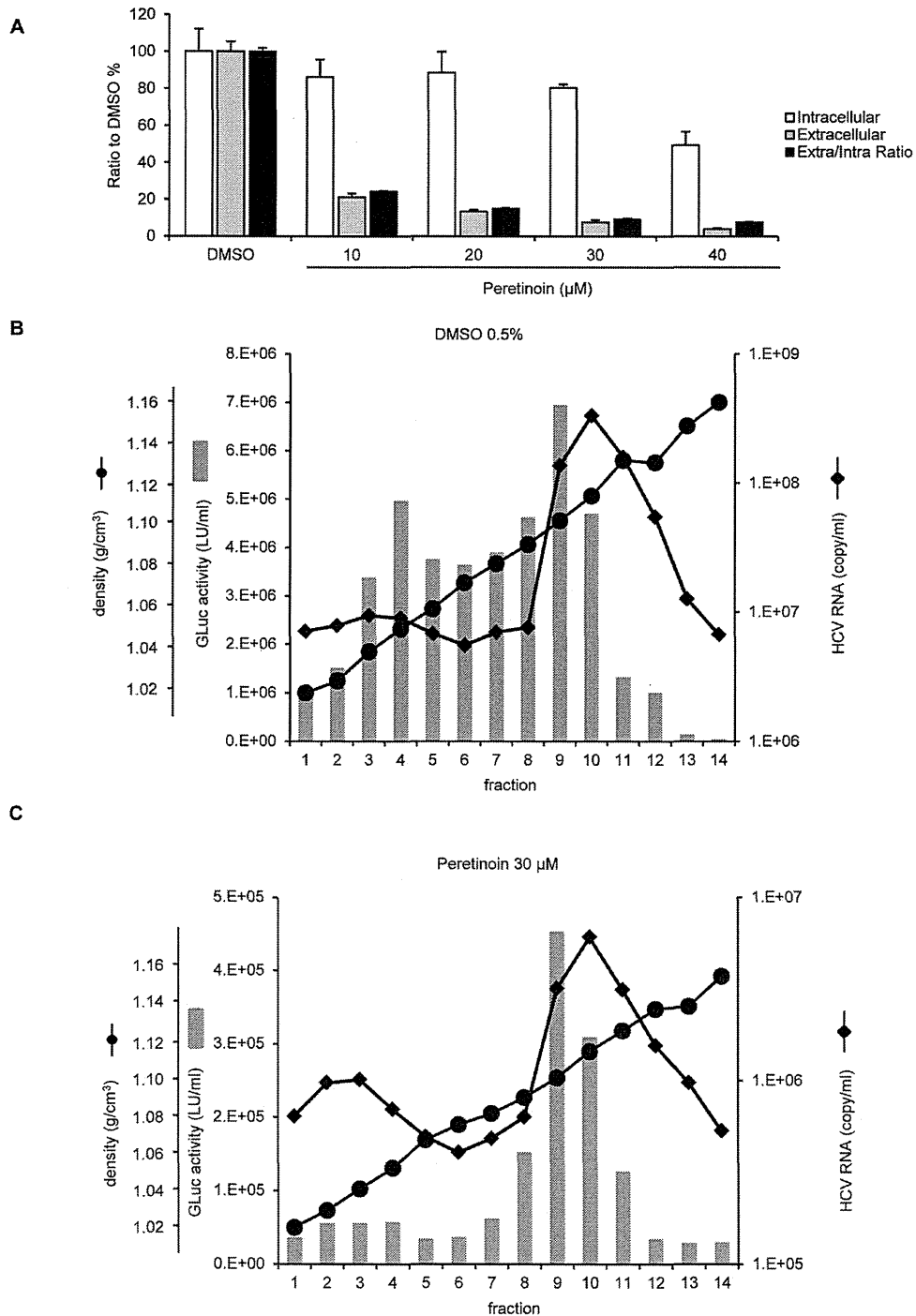


**Figure 6 | Impact of Peretinoin on infectious virus production.** (A) FT3-7 cells were transfected with HJ3-5/GLuc2A RNA, and 7 days later, 0.5% DMSO, or 10–40  $\mu\text{M}$  Peretinoin, were added. At 72 h later, extra- and intra-cellular viruses were collected and used to infect naïve Huh-7.5 cells. Replication capacity was also determined by measuring secreted GLuc activity. At 48 h after infection, we determined the amount of infectious virus from extra- and intra-cellular media by using GLuc activity as an indicator of the amount of infectious virus. Intra- and extra-cellular infectivity was normalised to replication capacity at infection, and these were then normalised to those of DMSO-treated cells, which were set to 100%. The ratio of extracellular infectious virus to intracellular virus was calculated at the indicated conditions, and it was then normalised to DMSO-treated cells, which were set to 100%. Data show the mean ratio to that of DMSO-treated cells  $\pm$  SD from 3 independent experiments. (B, C) FT3-7 cells were transfected with HJ3-5/GLuc2A RNA, and 7 days later, 0.5% DMSO or 30  $\mu\text{M}$  Peretinoin were added, and then 72 h later, the medium was collected and subjected to equilibrium ultracentrifugation. Fourteen fractions were taken and analysed for density (circles), HCV RNA levels (diamonds), and infectious virus titres determined by GLuc activity (grey bars). (B) shows the results from DMSO-treated cells, whilst (C) shows those for Peretinoin-treated cells.



suppress the growth of hepatoma cells, although the mechanism has not been fully understood. However, pharmacokinetic data from humans showed that the mean plasma concentration of lipid-bound Peretinoin is 7.3  $\mu\text{M}$  when patients received 600 mg Peretinoin daily for 8 weeks<sup>37</sup>. This concentration is very close to the antiviral EC<sub>50</sub> and could have an inhibitory effect on HCV replication, indicating that we could expect an antiviral effect at this dose in humans. Peretinoin showed an additive antiviral effect when combined with IFN $\alpha$ -2b (data not shown); furthermore, HCV did not acquire resistance to Peretinoin after 14 days treatment with 10–40  $\mu\text{M}$  Peretinoin (see Supplementary Fig. S11 online). Although it could be difficult to eradicate HCV only by Peretinoin due to its low selective index (CC50/EC50), combination therapy with Peretinoin plus PEG-IFN, ribavirin, or DAAs may further improve the SVR rate, as vitamin D has been proved to do<sup>38,39</sup>.

In summary, we have demonstrated that Peretinoin, which may in the future be administered to patients infected with HCV to prevent HCC, inhibits HCV RNA replication and infectious virus release by modifying several aspects of lipid metabolism.

## Methods

**Cell lines.** Huh-7.5 (kindly provided by Professor C. M. Rice, Rockefeller University, New York, NY), and FT3-7 cells (both clonal derivatives of Huh-7 cells) were maintained as described previously<sup>9</sup>. We used an immortalised human hepatocyte cell line, THLE-5b cells<sup>40</sup>, for the indicated experiments.

**Reagents.** Peretinoin and IFN $\alpha$ -2b were kindly provided by KOWA Company, Ltd. (Tokyo, Japan). ATRA, 9-cis RA, and 13-cis RA, were purchased from Sigma-Aldrich Japan K.K. (Tokyo, Japan). Stock solutions were prepared in DMSO, and all final dilutions contained 0.5% DMSO.

**Plasmids.** The GLuc coding sequence, followed by the FMDV2A sequence, was inserted between p7 and NS2 in pJFH1 and pHCV-N.2, which encode cDNA of genotype 2a JFH1<sup>13</sup> and genotype 1b N<sup>12</sup>, carrying several replication-enhancing mutations to be described elsewhere, respectively, by the same strategy adopted previously for H775<sup>10</sup>, pH77S.3/GLuc2A<sup>10</sup>, pHJ3-5/GLuc2A<sup>9</sup>, and pHJ3-5<sup>11</sup> have been described previously.

**Antiviral activity assay.** The indicated HCV RNAs were transfected by electroporation. The medium was replaced with fresh medium containing serial dilutions of the antiviral compounds at 48 h, and at 24 h intervals thereafter. Secreted GLuc activity was determined at 72 h after adding the antiviral compounds. The concentration of each compound required to reduce the amount of secreted GLuc activity by 50% (EC<sub>50</sub>) was determined using a 3-parameter Hill equation (Sigma Plot 10.0).

**Cell number determination.** Huh-7.5 cells were seeded in 96-well plates at a density of 5,000 cells/well, and at 24 h later, the indicated compounds were added. Cell numbers were determined by a WST-8 assay using Cell Counting Kit-8. The concentration of each compound required to reduce the amount of cell number by 50% (CC<sub>50</sub>) was determined using a 3-parameter Hill equation (Sigma Plot 10.0).

**RNA transcription.** HCV RNAs were synthesised using a MEGAScript T7 Kit, and synthesised RNA was purified using an RNeasy Mini Kit.

**Virus yield determination.** Huh-7.5 cells were seeded in 48-well plates at a density of 4.0  $\times 10^4$  cells/well at 24 h prior to inoculation with 100  $\mu\text{L}$  of virus-containing medium. The cells were maintained at 37°C in a 5% CO<sub>2</sub> environment and fed with 300  $\mu\text{L}$  medium at 24 h later. Following 48 h of additional incubation, the cells were fixed in methanol-acetone (1 : 1) at room temperature for 9 min and stained with a C7-50 monoclonal antibody to the HCV core protein (1 : 300). After extensive washing, the cells were stained with Alexa Fluor 568-conjugated anti-mouse IgG antibodies. A cluster of infected cells staining for core antigen was considered to constitute a single infectious FFU; virus titres are reported as FFUs/mL.

**Western blotting and immunostaining.** Western blotting and immunostaining were performed as described previously<sup>41,42</sup>. Briefly, the cells were washed in phosphate-buffered saline (PBS) and lysed in a radioimmunoprecipitation assay buffer containing complete Protease Inhibitor Cocktail and PhosSTOP. The membranes were blocked in Blocking One or Blocking One-P solution, and the expression of HCV core protein, FASN, precursor and mature SREBP1c, ApoE3, and  $\beta$ -actin was evaluated with mouse anti-core protein, rabbit anti-FASN, rabbit anti-SREBP1c, goat anti-ApoE3, and rabbit anti- $\beta$ -actin antibodies, respectively.

For immunofluorescence staining, the cells were washed twice with PBS and fixed in 4% paraformaldehyde for 15 min at room temperature. After washing again with PBS, the cells were permeabilised with 0.05% Triton X-100 in PBS for 15 min at room temperature. They were incubated in a blocking solution (10% foetal bovine serum

and 5% bovine serum albumin [BSA] in PBS) for 30 min, and then with the anti-core protein monoclonal antibodies. The fluorescent secondary antibodies were Alexa Fluor 568-conjugated anti-mouse IgG antibodies. Nuclei were labelled with DAPI, and LDs were visualised with BODIPY 493/503. Imaging was performed on a BIOREVO fluorescence microscope (Keyence Corporation, Osaka, Japan). The signal strength of LDs, core protein, and nuclei was quantitated by using Measurement Module BZ-H1M (Keyence Corporation).

**Quantitative RTD-PCR.** The primer pairs and probes for FASN and 18S rRNA were obtained from the TaqMan assay reagents library. HCV RNA was detected as described previously<sup>43</sup>.

**Secreted luciferase assay.** Cell culture supernatant fluids were collected at intervals after RNA transfection and the cells were re-fed fresh medium. Secreted GLuc was measured as described previously<sup>9</sup>.

**Fatty acid treatment and measurement of TGs.** The cells were treated with the indicated concentrations of OA in the presence of 2% fatty acid-free BSA. Intracellular TG content was measured using a TG Test according to the manufacturer's instructions.

**Intra- and extra-cellular infectivity assay.** To determine the amount of intra-cellular infectious virus, cell pellets of HJ3-5/GLuc2A-replicating FT3-7 cells harvested after trypsinization were resuspended in complete medium, washed twice with PBS, and lysed by 4 cycles of freezing and thawing. The lysates were clarified by centrifugation at 2,300  $\times g$  for 5 min prior to inoculation onto naïve Huh-7.5 cells. At the same time, extra-cellular medium was also collected. The medium derived from extra- and intra-cellular cultures was used to infect naïve Huh-7.5 cells, which were plated in 48-well plates at a density of 4.0  $\times 10^4$  cells/well at 24 h prior to infection. After 6 h inoculation, medium containing virus and possible carryover of Peretinoin was removed by extensive wash, and medium was replaced with fresh one every 24 h until 48 h. At 48 h after infection, we determined GLuc activity and used it as an indicator of the infectious virus titre.

**Equilibrium ultracentrifugation of HJ3-5/GLuc2A virus particles using an isopycnic iodixanol gradient.** Filtered supernatant fluids collected from HJ3-5/GLuc2A virus-replicating FT3-7 cells treated with DMSO or 30  $\mu\text{M}$  Peretinoin for 72 h were concentrated 30-fold using a Centricon PBHK Centrifugal Plus-20 Filter Unit with an Ultracel-PL membrane (100-kDa exclusion; Merck Millipore, Billerica, MA), then layered on top of a preformed continuous 10–40% iodixanol gradient in Hanks' balanced salt solution. The gradients were centrifuged in an SW41 rotor at 209,678  $\times g$  for 16 h at 4°C, and fractions (500  $\mu\text{L}$  each) were collected from the top of the tube. The density of each fraction was determined using a digital refractometer. Virus RNA was isolated from each gradient fraction using a QIAamp Viral RNA Kit, and cDNA was synthesised using a High Capacity cDNA Reverse Transcription Kit. RTD-PCR to quantitate the amount of HCV RNA was performed using a 7500 Real Time PCR System. Each fraction was used to infect naïve Huh-7.5 cells for 6 h, followed by extensive washing to ensure GLuc activity was reduced to background. The infected cells were inoculated and the medium was replaced with fresh medium every 24 h. GLuc activity, which was used as an alternative to the infectious virus titre, was determined at 72 h after infection.

1. Fried, M. W. *et al.* Peginterferon alfa-2a plus ribavirin for chronic hepatitis C virus infection. *N Engl J Med* **347**, 975–982 (2002).
2. Dabbouseh, N. M. & Jensen, D. M. Future therapies for chronic hepatitis C. *Nat Rev Gastroenterol Hepatol* **10**, 268–276 (2013).
3. Muto, Y. *et al.* Prevention of second primary tumors by an acyclic retinoid, polyphenolic acid, in patients with hepatocellular carcinoma. Hepatoma Prevention Study Group. *N Engl J Med* **334**, 1561–1567 (1996).
4. Muto, Y., Moriwaki, H. & Saito, A. Prevention of second primary tumors by an acyclic retinoid in patients with hepatocellular carcinoma. *N Engl J Med* **340**, 1046–1047 (1999).
5. Okada, H. *et al.* Acyclic retinoid targets platelet-derived growth factor signaling in the prevention of hepatic fibrosis and hepatocellular carcinoma development. *Cancer Res* **72**, 4459–4471 (2012).
6. Shimizu, M. *et al.* Acyclic retinoid inhibits diethylnitrosamine-induced liver tumorigenesis in obese and diabetic C57BLKS/J-/+ (db)/+Lepr(db) mice. *Cancer Prev Res* **4**, 128–136 (2011).
7. Morbitzer, M. & Herget, T. Expression of gastrointestinal glutathione peroxidase is inversely correlated to the presence of hepatitis C virus subgenomic RNA in human liver cells. *J Biol Chem* **280**, 8831–8841 (2005).
8. Yano, M. *et al.* Comprehensive analysis of the effects of ordinary nutrients on hepatitis C virus RNA replication in cell culture. *Antimicrob Agents Chemother* **51**, 2016–2027 (2007).
9. Shimakami, T. *et al.* Stabilization of hepatitis C virus RNA by an Ago2-miR-122 complex. *Proc Natl Acad Sci U S A* **109**, 941–946 (2012).
10. Shimakami, T. *et al.* Protease inhibitor-resistant hepatitis C virus mutants with reduced fitness from impaired production of infectious virus. *Gastroenterology* **140**, 667–675 (2011).



11. Yi, M., Ma, Y., Yates, J. & Lemon, S. M. Compensatory mutations in E1, p7, NS2, and NS3 enhance yields of cell culture-infectious intergenotypic chimeric hepatitis C virus. *J Virol* **81**, 629–638 (2007).
12. Beard, M. R. *et al.* An infectious molecular clone of a Japanese genotype 1b hepatitis C virus. *Hepatology* **30**, 316–324 (1999).
13. Wakita, T. *et al.* Production of infectious hepatitis C virus in tissue culture from a cloned viral genome. *Nat Med* **11**, 791–796 (2005).
14. Alvisi, G., Madan, V. & Bartenschlager, R. Hepatitis C virus and host cell lipids: an intimate connection. *RNA Biol* **8**, 258–269 (2011).
15. Bassendine, M. F., Sheridan, D. A., Bridge, S. H., Felmlee, D. J. & Neely, R. D. Lipids and HCV. *Semin Immunopathol* **35**, 87–100 (2013).
16. Herker, E. & Ott, M. Emerging role of lipid droplets in host/pathogen interactions. *J Biol Chem* **287**, 2280–2287 (2012).
17. Phan, T., Beran, R. K., Peters, C., Lorenz, I. C. & Lindenbach, B. D. Hepatitis C virus NS2 protein contributes to virus particle assembly via opposing epistatic interactions with the E1–E2 glycoprotein and NS3–NS4A enzyme complexes. *J Virol* **83**, 8379–8395 (2009).
18. Bocher, W. O., Wallasch, C., Hohler, T. & Galle, P. R. All-trans retinoic acid for treatment of chronic hepatitis C. *Liver Int* **28**, 347–354 (2008).
19. Bitetto, D. *et al.* Vitamin A deficiency is associated with hepatitis C virus chronic infection and with unresponsiveness to interferon-based antiviral therapy. *Hepatology* **57**, 925–933 (2013).
20. Hamamoto, S. *et al.* 9-cis retinoic acid enhances the antiviral effect of interferon on hepatitis C virus replication through increased expression of type I interferon receptor. *J Lab Clin Med* **141**, 58–66 (2003).
21. Masaki, T. *et al.* Interaction of hepatitis C virus nonstructural protein 5A with core protein is critical for the production of infectious virus particles. *J Virol* **82**, 7964–7976 (2008).
22. Miyanari, Y. *et al.* The lipid droplet is an important organelle for hepatitis C virus production. *Nat Cell Biol* **9**, 1089–1097 (2007).
23. Shimizu, Y. *et al.* Lipoprotein component associated with hepatitis C virus is essential for virus infectivity. *Curr Opin Virol* **1**, 19–26 (2011).
24. Collier, K. E. *et al.* Molecular determinants and dynamics of hepatitis C virus secretion. *PLoS Pathog* **8**, e1002466 (2012).
25. Hishiki, T. *et al.* Infectivity of hepatitis C virus is influenced by association with apolipoprotein E isoforms. *J Virol* **84**, 12048–12057 (2010).
26. Syed, G. H. & Siddiqui, A. Effects of hypolipidemic agent nordihydroguaiaretic acid on lipid droplets and hepatitis C virus. *Hepatology* **54**, 1936–1946 (2011).
27. Ploen, D. *et al.* TIP47 plays a crucial role in the life cycle of hepatitis C virus. *J Hepatol*, (2013).
28. Vogt, D. A. *et al.* Lipid Droplet-Binding Protein TIP47 Regulates Hepatitis C Virus RNA Replication through Interaction with the Viral NS5A Protein. *PLoS Pathog* **9**, e1003302 (2013).
29. Huang, J. T. *et al.* Hepatitis C Virus Replication Is Modulated by the Interaction of Nonstructural Protein NS5B and Fatty Acid Synthase. *J Virol* **87**, 4994–5004 (2013).
30. Fujino, T. *et al.* Expression profile of lipid metabolism-associated genes in hepatitis C virus-infected human liver. *Hepatol Res* **40**, 923–929 (2010).
31. Yang, W. *et al.* Fatty acid synthase is up-regulated during hepatitis C virus infection and regulates hepatitis C virus entry and production. *Hepatology* **48**, 1396–1403 (2008).
32. Lerat, H. *et al.* Hepatitis C virus proteins induce lipogenesis and defective triglyceride secretion in transgenic mice. *J Biol Chem* **284**, 33466–33474 (2009).
33. Waris, G., Felmlee, D. J., Negro, F. & Siddiqui, A. Hepatitis C virus induces proteolytic cleavage of sterol regulatory element binding proteins and stimulates their phosphorylation via oxidative stress. *J Virol* **81**, 8122–8130 (2007).
34. Muto, Y. & Moriwaki, H. Antitumor activity of vitamin A and its derivatives. *J Natl Cancer Inst* **73**, 1389–1393 (1984).
35. Suzui, M. *et al.* Growth inhibition of human hepatoma cells by acyclic retinoid is associated with induction of p21(CIP1) and inhibition of expression of cyclin D1. *Cancer Res* **62**, 3997–4006 (2002).
36. Nakamura, N. *et al.* Induction of apoptosis by acyclic retinoid in the human hepatoma-derived cell line, HuH-7. *Biochem Biophys Res Commun* **207**, 382–388 (1995).
37. Honda, M. *et al.* Peretinoin, an acyclic retinoid, improves the hepatic gene signature of chronic hepatitis C following curative therapy of hepatocellular carcinoma. *BMC cancer* **13**, 191 (2013).
38. Abu-Mouch, S., Fireman, Z., Jarchovsky, J., Zeina, A. R. & Assy, N. Vitamin D supplementation improves sustained virologic response in chronic hepatitis C (genotype 1)-naive patients. *World J Gastroenterol* **17**, 5184–5190 (2011).
39. Bitetto, D. *et al.* Vitamin D supplementation improves response to antiviral treatment for recurrent hepatitis C. *Transpl Int* **24**, 43–50 (2011).
40. Tokiwa, T. *et al.* Differentiation potential of an immortalized non-tumorigenic human liver epithelial cell line as liver progenitor cells. *Cell Biol Int* **30**, 992–998 (2006).
41. Shirasaki, T. *et al.* La protein required for internal ribosome entry site-directed translation is a potential therapeutic target for hepatitis C virus replication. *J Infect Dis* **202**, 75–85 (2010).
42. Shirasaki, T. *et al.* MicroRNA-27a Regulates Lipid Metabolism and Inhibits Hepatitis C Virus Replication in Human Hepatoma Cells. *J Virol* **87**, 5270–5286 (2013).
43. Honda, M., Shimazaki, T. & Kaneko, S. La protein is a potent regulator of replication of hepatitis C virus in patients with chronic hepatitis C through internal ribosomal entry site-directed translation. *Gastroenterology* **128**, 449–462 (2005).

## Acknowledgments

We would like to thank Dr T. Wakita (National Institute of Infectious Disease, Tokyo, Japan) for providing the plasmid encoding JFH1, Dr C. Lee (ThinkSCIENCE INC., Tokyo, Japan) for assistance for medical writing and proof-reading, and Ms Y. Terao (Kanazawa University Hospital, Kanazawa, Japan) for making illustrations. This work was partially supported by the Takeda Science Foundation.

## Author contributions

Study design and concept; T.S., T.S. and D.Y., Acquisition of data; T.S., T.S., F.L., K.M., T.S., R.T. and M.F., Drafting of the manuscript; T.S. and T.S., Critical revision of the manuscript for important intellectual content; M.H., D.Y., S.M., S.L. and S.K., Study supervision; M.H. and S.K. All authors reviewed the manuscript.

## Additional information

Supplementary information accompanies this paper at <http://www.nature.com/scientificreports>

**Competing financial interests:** The authors declare no competing financial interests.

**How to cite this article:** Shimakami, T. *et al.* The Acyclic Retinoid Peretinoin Inhibits Hepatitis C Virus Replication and Infectious Virus Release *in Vitro*. *Sci. Rep.* **4**, 4688; DOI:10.1038/srep04688 (2014).



This work is licensed under a Creative Commons Attribution-NonCommercial-NoDerivs 3.0 Unported License. The images in this article are included in the article's Creative Commons license, unless indicated otherwise in the image credit; if the image is not included under the Creative Commons license, users will need to obtain permission from the license holder in order to reproduce the image. To view a copy of this license, visit <http://creativecommons.org/licenses/by-nc-nd/3.0/>

# In vivo immunological antitumor effect of OK-432-stimulated dendritic cell transfer after radiofrequency ablation

Hidetoshi Nakagawa · Eishiro Mizukoshi · Noriho Iida · Takeshi Terashima · Masaaki Kitahara · Yohei Marukawa · Kazuya Kitamura · Yasunari Nakamoto · Kazumasa Hiroishi · Michio Imawari · Shuichi Kaneko

Received: 1 June 2013 / Accepted: 17 December 2013 / Published online: 3 January 2014  
© Springer-Verlag Berlin Heidelberg 2013

**Abstract** Radiofrequency ablation therapy (RFA) is a radical treatment for liver cancers and induces tumor anti-gen-specific immune responses. In the present study, we examined the antitumor effects of focal OK-432-stimulated dendritic cell (DC) transfer combined with RFA and analyzed the functional mechanisms involved using a murine model. C57BL/6 mice were injected subcutaneously with colon cancer cells (MC38) in their bilateral flanks. After the establishment of tumors, the subcutaneous tumor on one flank was treated using RFA, and then OK-432-stimulated DCs were injected locally. The antitumor effect of the treatment was evaluated by measuring the size of the tumor on the opposite flank, and the immunological responses were assessed using tumor-infiltrating lymphocytes, splenocytes and draining lymph nodes. Tumor growth was strongly inhibited in mice that exhibited efficient DC migration after RFA and OK-432-stimulated DC transfer, as compared to

mice treated with RFA alone or treatment involving immature DC transfer. We also demonstrated that the antitumor effect of this treatment depended on both CD8-positive and CD4-positive cells. On the basis of our findings, we believe that combination therapy for metastatic liver cancer consisting of OK-432-stimulated DCs in combination with RFA can proceed to clinical trials, and it is anticipated to be markedly superior to RFA single therapy.

**Keywords** Metastatic liver cancer · MC38 · Immunotherapy · Intratumoral injection · Tumor-infiltrating lymphocyte

## Abbreviations

RFA	Radiofrequency ablation
DC	Dendritic cell
HCC	Hepatocellular carcinoma
TAE	Transcatheter hepatic arterial embolization
TLR	Toll-like receptor
GFP	Green fluorescent protein
ELISPOT	Enzyme-linked immunospot
Treg	Regulatory T cell
MDSC	Myeloid-derived suppressor cell
IFN- $\gamma$	Interferon- $\gamma$

**Electronic supplementary material** The online version of this article (doi:10.1007/s00262-013-1514-7) contains supplementary material, which is available to authorized users.

H. Nakagawa · E. Mizukoshi · N. Iida · T. Terashima · M. Kitahara · Y. Marukawa · K. Kitamura · S. Kaneko (✉)  
Disease Control and Homeostasis, Graduate School of Medical Sciences, Kanazawa University, 13-1 Takara-machi, Kanazawa, Ishikawa 920-8641, Japan  
e-mail: skaneko@m-kanazawa.jp

H. Nakagawa  
e-mail: hidetoshi.naka@gmail.com

Y. Nakamoto  
Second Department of Internal Medicine, Faculty of Medical Sciences, University of Fukui, Fukui 910-1193, Japan

K. Hiroishi · M. Imawari  
Shin-yurigaoka General Hospital, Kawasaki, Kanagawa 215-0026, Japan

## Introduction

Liver is one of the most common organs to which various cancers spread from their site of origin. In some types of cancer, the liver metastasis lesion is a target of surgical treatment. For instance, surgical resection of hepatic metastasis achieves longer median survival in colorectal and breast cancer patients [1, 2]. However, even if the hepatic lesions are surgically treated, the prognosis of the

patients is not satisfactory. As for colorectal cancers, the recurrence rate is over 50 % after radical resection of metastatic lesions [3]. Moreover, at the time of initial diagnosis, only a few patients meet the criteria for hepatic resection because of unresectability, low hepatic functional reserve or poor performance status [4].

Radiofrequency ablation therapy (RFA) has been developed as a radical and minimally invasive treatment method for metastatic liver cancers. Recently, RFA has been used as an adjunct to hepatic resection or as an alternative method to resection when surgical treatment is not feasible [5]. Additionally, it has been revealed that RFA for metastatic liver cancers generates tumor antigen-specific T-cell responses in man [6, 7]. We have previously reported that RFA could also control distant tumor growth in a murine hepatocellular carcinoma (HCC) model [8].

Dendritic cells (DCs) are potent antigen-presenting cells [9]. Recently, we have established new treatments using local DC injection with transcatheter hepatic arterial embolization (TAE) and have shown that this combination therapy could induce tumor antigen-specific T-cell responses in HCC patients [10].

OK-432 is derived from the Su strain of Group A *Streptococcus pyogenes* by means of treatment with benzylpenicillin and heat [11]. OK-432 can stimulate DCs via Toll-like receptor (TLR) 3, TLR4 and  $\beta$ 2 integrin and subsequently induce antigen-specific cytotoxic lymphocytes [12–14].

On the basis of these results, we hypothesized that OK-432-stimulated DC transfer is a promising candidate for an enhancer that can strongly increase the antitumor effect of RFA. We have previously demonstrated in a clinical trial that the local infusion of OK-432-stimulated DC after TAE could prolong recurrence-free survival in HCC patients [15]. However, it remains unknown as to how the transferred DCs work in combination with RFA. In the present study, we examined the antitumor effects of OK-432-stimulated DCs when combined with RFA and analyzed the functional mechanisms involved using a murine subcutaneous colon cancer model.

## Materials and methods

### Animals

Wild-type 8–12-week-old female C57BL/6 J mice were obtained from Charles River Japan (Yokohama, Japan). Female C57BL/6-Tg (UBC-GFP) 30Scha/J mice were purchased from the Jackson Laboratory (Bar Harbor, ME, USA). All animal experiments were approved and performed in accordance with the Guidelines for the Care and Use of Laboratory Animals of Kanazawa University, which

strictly conforms to the Guide for the Care and Use of Laboratory Animals published by the US National Institutes of Health.

### Cell lines and bone marrow-derived dendritic cells

A murine colorectal cancer cell line, MC38 and hybridomas, clone GK1.5 and clone 2.43 were cultured in RPMI-1640 containing 10 % fetal bovine serum (Life Technologies, Co., Carlsbad, CA, USA) supplemented with 100  $\mu$ g/ml streptomycin and 100 units/ml penicillin (Wako Pure Chemical Industries Ltd., Osaka, Japan). Bone marrow-derived dendritic cells (BMDCs) were generated using 20 ng/ml of recombinant granulocyte macrophage colony-stimulating factor (R&D Systems, Minneapolis, MN, USA) as previously described [16]. OK-432 (Picibanil; Chugai Pharmaceutical Co. Ltd., Tokyo, Japan) was loaded into the supernatant from days 6–7 of the BMDC generation period at a concentration of 5  $\mu$ g/ml.

### In vitro evaluation of phagocytic activity by dendritic cells

MC38 cells were labeled with DiD dye (Life Technologies) according to the manufacturer's instructions followed by heat treatment at 80 °C for 90 s. OK-432-stimulated or immature DCs were co-incubated with the treated MC38 cells for 3 h at a ratio of 1:1. After incubation, the cell suspensions were observed using a fluorescence microscope (BZ9000: Keyence, Osaka, Japan) and analyzed by means of FACSCalibur (BD Immuno-Cytometry System, San Jose, CA, USA).

### Animal model

Bilateral flanks of C57BL/6 mice were each injected subcutaneously with  $1 \times 10^6$  MC38 cells. Seven days after injection, after they had grown to 5–6 mm in diameter, the subcutaneous tumors on one flank were treated using RFA, and  $1 \times 10^7$  immature DCs or  $1 \times 10^7$  OK-432-stimulated DCs were injected into the treated tumors at 24 h after RFA. After this, the volume of the untreated tumor on the contralateral flank was evaluated over a period of 10 days. Tumor volumes were calculated using the following formula: tumor volume ( $\text{mm}^3$ ) = (longest diameter)  $\times$  (shortest diameter)<sup>2</sup>/2.

### Radiofrequency ablation

Mice bearing tumors were anesthetized with an intraperitoneal injection of pentobarbital (Kyoritsu Seiyaku, Tokyo, Japan), and the skin on the tumor was cut. Subsequently, an expandable RFA needle was inserted into the tumor, which was treated using a radiofrequency generator (RITA

500PA; RITA Medical Systems, Inc., Fremont, CA, USA). During the use of this system, the intratumor temperature was maintained at 70–90 °C, and the current was turned off when the tumor exhibited heat denaturation.

#### Flow cytometry

The DCs were detected by means of staining with anti-CD11c antibodies (Life technologies). The lymphocytes in the draining lymph node were stained with anti-CD4 antibodies, anti-CD8 antibodies, anti-CD11c antibodies and anti-CD69 antibodies (BD Bioscience, San Diego, CA, USA). The splenocytes were stained with anti-CD4 antibodies, anti-CD8 antibodies, CD11c antibodies, anti-NK1.1 antibodies, CD45 antibodies (BD Bioscience), anti-Gr-1 antibodies, and anti-CD11b antibodies and mouse regulatory T-cell staining solution (BioLegend, San Diego, CA, USA). The stained samples were analyzed using FACS Aria II (BD Immuno-Cytometry System).

#### Immunohistochemical assay

The draining lymph nodes and the observed tumors were embedded in Sakura Tissue-Tek optimum cutting temperature compound (Sakura Finetek Japan Co., Ltd., Tokyo, Japan) for frozen sectioning. Tissue sections were fixed at –20 °C in methanol for 10 min. The draining lymph nodes were stained using rabbit anti-GFP antibody (Abcam, Cambridge, UK) that were detected using an EnVision+/HRP kit (Dako, Glostrup, Denmark). The observed tumors were stained with anti-CD4 and anti-CD8a (BD Bioscience), which were detected using the Nichirei Histofine Simple Stain Mouse Max PO (Rat) system (Nichirei Co., Tokyo, Japan) or the Vectastain ABC kit (Vector Laboratory, Inc., Burlingame, CA, USA).

#### Interferon gamma enzyme-linked immunospot assay

The splenocytes, the tumor-infiltrating lymphocytes (TILs) in the untreated tumors that were isolated by mechanical homogenizations and density gradient centrifugations, and the lymphocytes in the draining lymph nodes were loaded into the interferon gamma enzyme-linked immunospot assay to estimate the tumor-specific immune reactions, as previously described [8, 17]. Briefly,  $3 \times 10^5$  lymphocytes or  $1 \times 10^5$  TILs were incubated for 24 h with or without  $6 \times 10^5$  MC38 lysates, which were prepared through five cycles of rapid freezing in liquid nitrogen, thawing at 55 °C and centrifugation. The number of MC38-specific IFN- $\gamma$  spots was determined by subtracting the number of spots incubated without MC38 lysates from the number of spots incubated with MC38 lysates. For CD4 or CD8 depletion,

we used magnetic CD4 beads or CD8 beads (Miltenyi Biotec, Bergisch Gladbach, Germany).

#### In vivo CD4/CD8 depletion

For in vivo CD4 or CD8 depletion, B6 mice were injected intraperitoneally with 200  $\mu$ g of purified monoclonal antibodies specific to CD4 or CD8 at 1 day before and 3 days after RFA treatment; the monoclonal antibodies were prepared from GK1.5 hybridoma and 2.43 hybridoma, respectively [18]. The depletion was confirmed by flow cytometry using peripheral blood lymphocytes stained with anti-CD4 and anti-CD8 antibodies.

#### Statistical analysis

The data obtained were analyzed statistically using the *t* test or one-way analysis of variance followed by Tukey's multiple-comparison test. A *P* value <0.05 was considered as being statistically significant.

## Results

#### Migration efficacy and phagocytic ability of OK-432-stimulated DCs

We employed OK-432 as a modifying agent for DCs, because we have previously shown in clinical studies that OK-432 prolonged recurrence-free survival after combination therapy involving DC injection with TAE for HCC patients [10, 15]. We first confirmed that the OK-432-stimulated murine DCs showed higher expression of maturation markers such as CD40, CD80, CD86, MHC class II and CCR7 (Supplementary Fig. 1), as previously reported [19, 20].

To evaluate their phagocytic abilities, we incubated the immature DCs and the OK-432-stimulated DCs with MC38 tumor cells. Heat-treated MC38 cells were taken up well by both immature DCs and OK-432-stimulated DCs, as compared to nontreated MC38 cells (Fig. 1a–c). In addition, the phagocytic ability of OK-432-stimulated DCs was not inferior to that of immature DCs. These results were consistent with the dextran uptake assay (Supplementary Fig. 2) and our previous data on human monocyte-derived DCs [15]. Since heat-treated MC38 cells were thought to be in a similar condition to those in the MC38 tumor in mice treated with RFA, OK-432-stimulated DCs were expected to effectively phagocytose RFA-treated MC38 tumor cells in vivo.

We next estimated the kinetics of the transferred DCs in mice bearing subcutaneous MC38 tumors treated with RFA. Immature DCs or OK-432-stimulated DCs that were derived from GFP-Tg mice were injected intratumorally

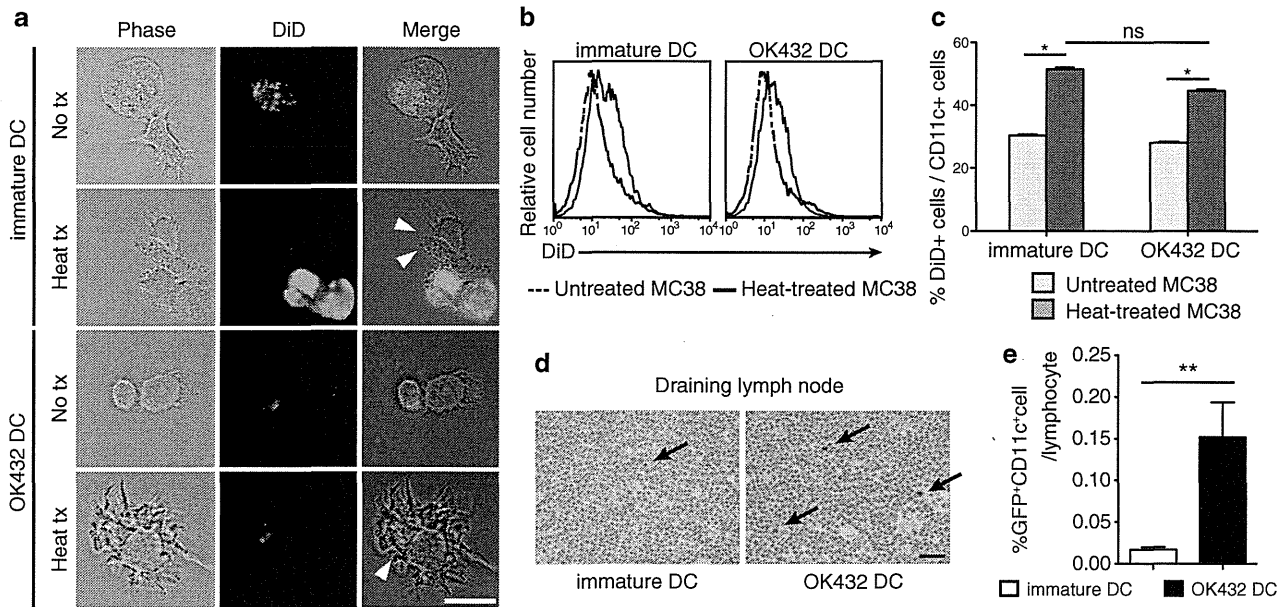


**Fig. 1** Effects of OK-432 on murine bone marrow-derived DCs. **a** OK-432-stimulated DCs or immature DCs were co-incubated for 3 h with MC38 cells untreated or treated at 80 °C for 90 s after staining with DiD dye. After incubation, DC and MC38 cells were observed using a fluorescence microscope. *Arrowheads* indicate MC38 derivatives being phagocytosed by DCs. No tx, untreated MC38 cells; heat tx, heat-treated MC38 cells; *bar*, 20  $\mu$ m. **b**, **c** Co-incubated MC38 cells and DCs were stained with anti-CD11c antibodies and analyzed using flow cytometry. The *histograms* show the DiD fluorescent intensity of the CD11c-positive fractions. The percentages of DiD<sup>+</sup> CD11c<sup>+</sup> cells in the CD11c<sup>+</sup> cell population are also shown in a *col-*

*umn graph*. The experiments were performed five times, and representative results are shown. Data are presented as the mean  $\pm$  SE. \* $P < 0.05$ . **d** The migration abilities of the DCs after intratumoral transfer were evaluated. The draining lymph nodes were harvested at 3 days after RFA followed by the DC transfer. Frozen sections were prepared and stained with anti-GFP antibodies. *Arrows* indicate the GFP-positive cells in the lymph nodes. *Bar* 20  $\mu$ m. **e** The draining lymph nodes were also analyzed using flow cytometry after staining with anti-CD11c antibodies. Data were obtained from six mice in each group. Percentages of GFP<sup>+</sup> CD11c<sup>+</sup> cell are presented as the mean  $\pm$  SE. \*\* $P < 0.01$

at 24 h after RFA treatment, and the subcutaneous tumors and the lymph nodes were harvested at 3 days after RFA. According to the immunohistochemical study involving the detection of GFP, the inguinal lymph node on the RFA-treated flank was thought to be the draining lymph node (Supplementary Fig. 3). Additionally, the number of transferred DCs in the draining lymph nodes was significantly higher in the mice treated with the OK-432-stimulated DCs than in those treated with the immature DCs (Fig. 1d, e). Our experimental results attested to the fact that the OK-432-stimulated DCs had both sufficient phagocytic ability and higher migration efficacy.

#### Effect of RFA in combination with the injection of OK-432-stimulated DCs on tumor growth

OK-432-stimulated DCs were used in combination therapy with RFA in this murine model (Fig. 2a). Namely, BMDCs stimulated with OK-432 were injected into RFA-treated tumor at 24 h after RFA treatment. We compared four groups of tumor-bearing mice as follows: (1) no treatment; (2) RFA only; (3) RFA with the injection of immature DCs; and (4) RFA with the injection of OK-432-stimulated

DCs. Tumor volumes were measured for 10 days after treatment/no treatment. On the day after RFA, the treated tumors were covered with scars, started to shrink and had disappeared macroscopically at 4 days after RFA in all of the groups. This indicated that RFA treatment was highly effective for focal lesions. The injected DCs were detected in the treated tumors (Supplementary Fig. 3). With regard to the untreated tumors, as we previously reported, the group treated with RFA only showed an antitumor effect against distant tumors. The injection of immature DCs combined with RFA did not show any additional enhancement of the antitumor effect. On the other hand, the volumes of the untreated tumors in the group that underwent RFA combined with the injection of OK-432-stimulated DCs were strongly suppressed ( $P < 0.001$ ) relative to other groups (Fig. 2b).

#### Recruitment of antigen-specific lymphocyte fractions in both splenocytes and tumor by injected OK-432-stimulated DCs

Ten days after RFA, the tumors and the spleens were harvested and analyzed using immunohistochemical staining.

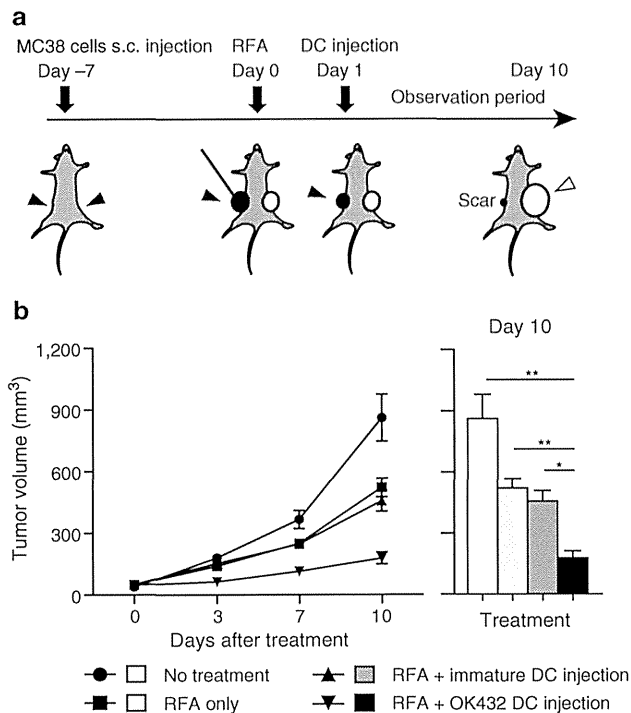


**Fig. 2** Impact of injection of OK-432-stimulated DCs into murine MC38 subcutaneous tumors. **a** RFA was administered to a tumor on one flank followed by injection of  $1 \times 10^7$  DCs into the treated tumor. The untreated tumor on the opposite flank was observed for 10 days. The *solid arrowheads* indicate the treatment intervention sites, and the *open arrowhead* indicates the observed untreated tumor. **b** The tumor volumes were compared among the four groups as follows: (1) no treatment; (2) RFA only; (3) RFA in combination with immature DC injection; and (4) RFA in combination with OK-432-stimulated DC injection.  $n = 8$  mice per group. The data are presented as the mean  $\pm$  SE. \* $P < 0.05$ ; \*\* $P < 0.001$

We examined the number of tumor-infiltrating CD4-positive or CD8-positive cells in the tumors by means of immunohistochemistry. The infiltration of these cells into the untreated tumors was found to be promoted by RFA. The injection of OK-432-stimulated DCs after RFA induced the additional recruitment of CD8-positive cells into the untreated tumors (Fig. 3a, b). CD11c-, CD11b- and NK1.1-positive cells were very marginal and showed no differences in number among the four groups (data not shown).

Systemically, in terms of analyzing splenocytes with flow cytometry, the number of CD4-positive and CD8-positive cells increased in the group treated with RFA in combination with OK-432-stimulated DCs. On the other hand, the CD11c and NK1.1 fractions, which were considered as DCs and NK cells, respectively, presented no difference among the four groups (Fig. 3c). In addition, we examined the effect of the injection of OK-432-stimulated DCs after RFA on inhibitory blood cells such as regulatory T cells (Tregs) and myeloid-derived suppressor cells (MDSCs) (Fig. 3c). Among CD4-positive cells, significantly fewer

Tregs were detected in the group treated with RFA in combination with OK-432-stimulated DCs than in the group treated with RFA in combination with immature DCs. In the analysis of MDSCs, their rates of occurrence were not affected by treatment with either RFA alone or RFA in combination with DCs. Taking these results together, we concluded that treatment with RFA combined with OK-432-stimulated DCs enhanced the number of CD4- or CD8-positive T cells and reduced the Treg/CD4 ratio, but did not influence MDSC numbers.

Furthermore, we examined the number of tumor-specific IFN- $\gamma$ -producing cells at 10 days after RFA using the ELISPOT assay. The number of IFN- $\gamma$ -producing cells among splenocytes and TILs showed the same trend as the level of tumor growth control among the four groups (Fig. 3d); the group treated with RFA in combination with injected OK-432 DCs showed the most abundant specific spots. These results suggested that the augmented antitumor effects of RFA combined with OK-432-stimulated DCs depended in large part on tumor-specific immune responses by CD4 cells or CD8 cells.

#### Evaluation of tumor-specific immune responses in the draining lymph node after OK-432-stimulated DC transfer

CD4 T cells and CD8 T cells are now thought to have an important antitumor effect as a result of the OK-432-stimulated DC transfer. To elucidate the priming of the antigen-specific immune response, we analyzed the draining lymph nodes at 3 days after RFA focusing on CD4-positive or CD8-positive cells. CD69, the early activation marker, on CD4-positive and CD8-positive cells was examined and compared between the immature DC transfer group and the OK-432-stimulated DC transfer group. It was found that CD69 expression on both CD4-positive and CD8-positive cells was elevated in the OK-432-stimulated DC transfer group (Fig. 4a, b). The activations were also demonstrated to be tumor-specific using the IFN- $\gamma$  ELISPOT assay in which each of CD4-negative and CD8-negative fractions was applied to the assay and both showed tumor-specific IFN- $\gamma$  secretions (Fig. 4c).

#### Evaluation of the relationship between CD4-positive and CD8-positive cells and the antitumor effects of RFA and OK-432-stimulated DC transfer

We have demonstrated that combination therapy involving RFA and OK-432-stimulated DC transfer might generate enhanced antitumor effects via tumor-specific CD4-positive and CD8-positive cells. To obtain further evidence, we carried out in vivo CD4 or CD8 depletion studies in mice. Initially, we confirmed CD4 or CD8 depletion in the control in vivo study (Supplementary Fig. 4). The



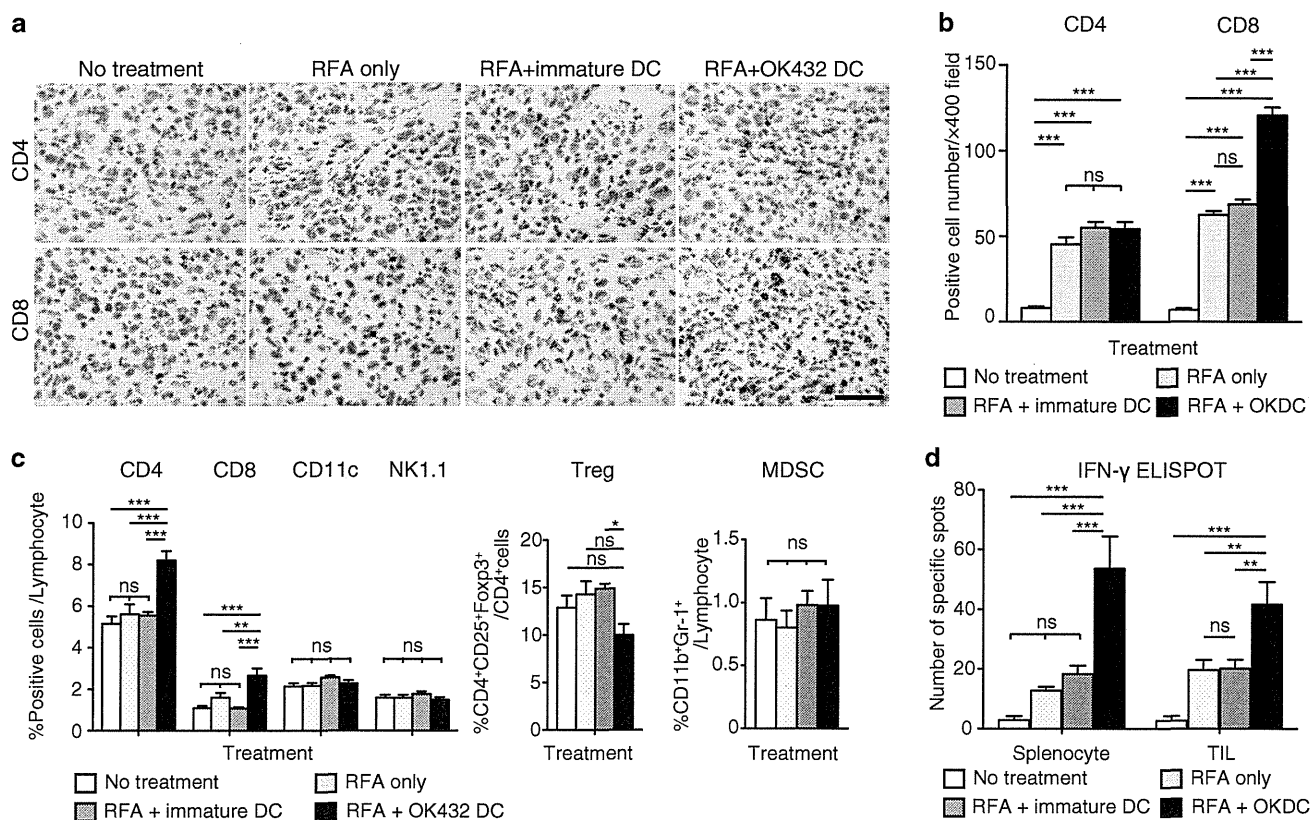


**Fig. 3** Analysis of the tumor-infiltrating lymphocytes and the splenocytes after combination therapy with RFA and DC injection. **a** CD4-positive and CD8-positive cells in the observed untreated tumors were detected using immunohistochemistry at 10 days after RFA. The *black bar* represents 50  $\mu$ m. **b** The number of positive cells was counted using a microscope. This was achieved by counting the number of cells in six randomly chosen tumor areas at 400-fold magnification. Three mice were used in each group. The data are presented as the mean  $\pm$  SE. \*\*\*  $P < 0.001$ ; *ns* not significant. **c** Ten days after RFA, splenocytes were stained with anti-CD4, anti-CD8, anti-NK1.1 and anti-CD11c antibodies and analyzed using flow cytometry. Regulatory T cells (Tregs) defined as CD4<sup>+</sup>CD25<sup>+</sup>Foxp3<sup>+</sup>

cells and myeloid-derived suppressor cells (MDSCs) defined as CD11b<sup>+</sup>Gr-1<sup>+</sup> cells were counted and compared among the four groups. Six mice were analyzed in each group. The data are presented as the mean  $\pm$  SE. \* $P < 0.05$ ; \*\* $P < 0.01$ ; \*\*\* $P < 0.001$ ; *ns* not significant. **d** Immune responses by the splenocytes and the tumor-infiltrating lymphocytes (TILs) were examined by means of the IFN- $\gamma$  enzyme-linked immunospot (ELISPOT) assay using MC38 lysate. In the assay for TILs,  $1 \times 10^5$  TILs were mixed with  $2 \times 10^5$  splenocytes from B6 mice and applied to the well. Six mice were analyzed in each group. The data are presented as the mean  $\pm$  SE. \*\* $P < 0.01$ ; \*\*\* $P < 0.001$ ; *ns* not significant

CD4-positive and CD8-positive fractions in the peripheral blood were greatly depleted at 7 days after injection of the antibodies. The experimental schedule was determined as follows. The depletion antibodies were injected at 1 day before and 3 days after RFA, and the tumors that were not treated with RFA were observed for 10 days. In addition, the draining lymph nodes were harvested at 3 days after RFA and analyzed (Supplementary Fig. 5). The antitumor effects of RFA treatment and the augmented effects from OK-432-stimulated DCs were cancelled out by depletion of both CD4 and CD8 cells (Fig. 5a). In the CD4 depletion study, there was no priming of the antitumor effect in the draining lymph nodes (Fig. 5b; Supplementary Fig. 6). On the other hand, in the CD8 depletion study CD4 cells were activated with tumor specificities in the draining lymph node in both groups, and the activation was stronger in the

OK-432-stimulated DC transfer group (Fig. 5b; Supplementary Fig. 6). Tumor-specific reactions were also demonstrated in the splenocytes and the TILs at 10 days after RFA. There was a tendency for OK-432 DC transfer treatment to result in the recruitment of increased numbers of tumor-specific lymphocytes into the tumor on the opposite flank ( $P = 0.184$ ; Fig. 5c). These results indicated that the tumor-specific activation of CD8 cells was necessary for the antitumor effect and was completely dependent on help from the CD4 cells.

## Discussion

In the past decade, cytotoxic agents and molecular-targeted therapies have been developed, and the treatment outcomes

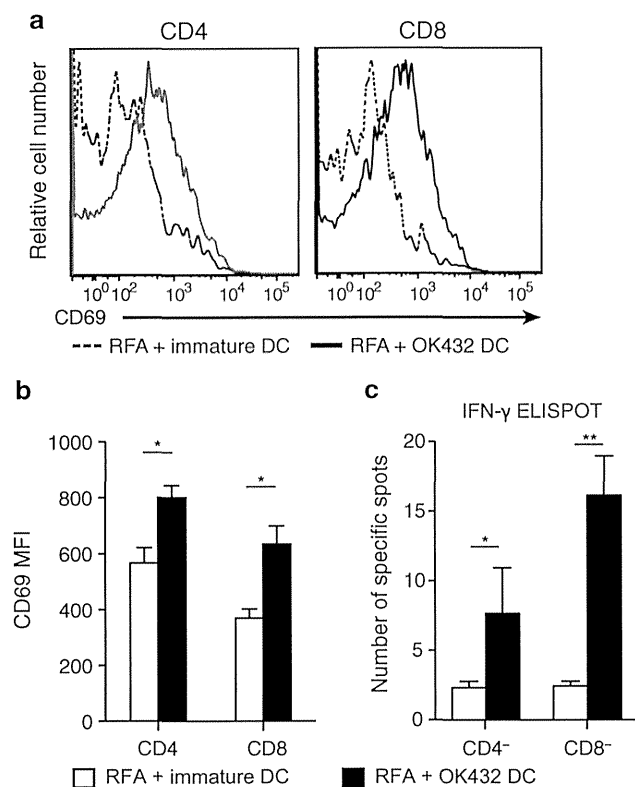


**Fig. 4** Antigen-specific activation of both CD4-positive and CD8-positive cells in the draining lymph node. **a** Three days after RFA followed by DC transfer, the draining lymph node was harvested and analyzed by staining with anti-CD4 antibodies, anti-CD8 antibodies and anti-CD69 antibodies. The fluorescence intensities of CD69 in the CD4-positive and CD8-positive fractions are compared between the OK-432-stimulated DC transfer group and the immature DC transfer group. The data were obtained from six mice in each group. The histograms show the representative data. **b** The mean fluorescent intensities are also presented as the mean  $\pm$  SE. \* $P < 0.05$ . **c** The antigen specificities of the T-cell activations were confirmed by means of the IFN- $\gamma$  ELISPOT assay using MC38 lysate. After CD4 or CD8 depletion using CD4 and CD8 magnetic beads, the lymphocytes from the draining lymph nodes were submitted to IFN- $\gamma$  ELISPOT assay. Data were obtained from six mice in each group. \* $P < 0.05$ ; \*\* $P < 0.01$

for various cancers have improved. However, few patients with advanced cancers have been completely cured, and thus, new strategies for anticancer therapy are required. Immunotherapy is considered to have the potential to effectively treat such advanced cancers, and many different approaches have been explored. For the utilization of the adoptive immune response in a cancer therapy, DCs are a key constituent of the immune system. This is because of their natural potential to present tumor-associated antigens to CD4<sup>+</sup> and CD8<sup>+</sup> lymphocytes and also to control both immune tolerance and immunity [21]. Thus, DCs are considered as an important target for cancer immunotherapy. Many trials and studies have been carried out regarding

immunotherapy for cancer using DCs, some of which have been reported to have pronounced effects [22–25]. In recent studies, it has been revealed that RFA treatment induces tumor-specific T-cell responses, which is known as the abscopal effect; this has been mainly reported in radiotherapy studies and is augmented with combined immunotherapies [26, 27]. Brok et al. [28] have previously reported on the vaccination effects of combination therapy involving RFA and CTLA-4 antibody.

To our knowledge, this is the first study that has demonstrated using a murine metastatic cancer model that RFA in combination with focal DC injection could enhance the antitumor effects of RFA alone. Our results showed that immature DCs made no additional immunological contribution to RFA. In the analysis of draining lymph nodes, few transferred DCs were detected after the injection of immature DCs. It appeared that immature DCs did not act as sentinels in the adoptive immune system, partially because they exhibited low expression of CCR7 (the main molecule that promotes DC migration [29]), even though elevation of CCR7 expression using OK-432 was very modest in our study. There is another possibility immature DCs are easily lysed and excluded by the host immune system [30]. On the other hand, mature DCs can escape cell lysis [31].

Utilization of OK-432-stimulated DCs improved the number of migrating transferred DCs in the present study. These DCs, which could act as sentinels for immunity, induced expansion in the number of tumor-specific lymphocytes in the draining lymph nodes, in the splenocytes and in the distant nontreated tumors, without systemic expansion of inhibitory cells such as Tregs or MDSCs. We also demonstrated that these augmented antitumor effects after OK-432-stimulated DC transfer were primed in the draining lymph nodes with tumor-specific activations of CD4-positive and CD8-positive cells; it was proved that without CD4-positive or CD8-positive cells, both the antitumor effect by RFA and the additional effect of the injection of OK-432-stimulated DCs disappeared completely. In addition, the *in vivo* CD4 depletion study revealed that tumor-specific activations of CD8-positive cells were not seen in the draining lymph nodes in both groups after the injection of immature DCs and OK-432-stimulated DC injection; in other words, tumor-specific CD8 activation depended on CD4-positive cells entirely. In the CD8 depletion study, on the other hand, we found that tumor-specific CD4-positive cells appeared in the draining lymph nodes, the splenocyte population and the untreated tumor on the opposite flank, and these lymphocytes were considered to be CD4-positive cells. In the tumor-infiltrating lymphocytes, there was a tendency for more tumor-specific CD4-positive cells to be recruited after treatment involving OK-432-stimulated DC transfer. Many researchers have demonstrated the contribution of CD4 cells to cytotoxicity

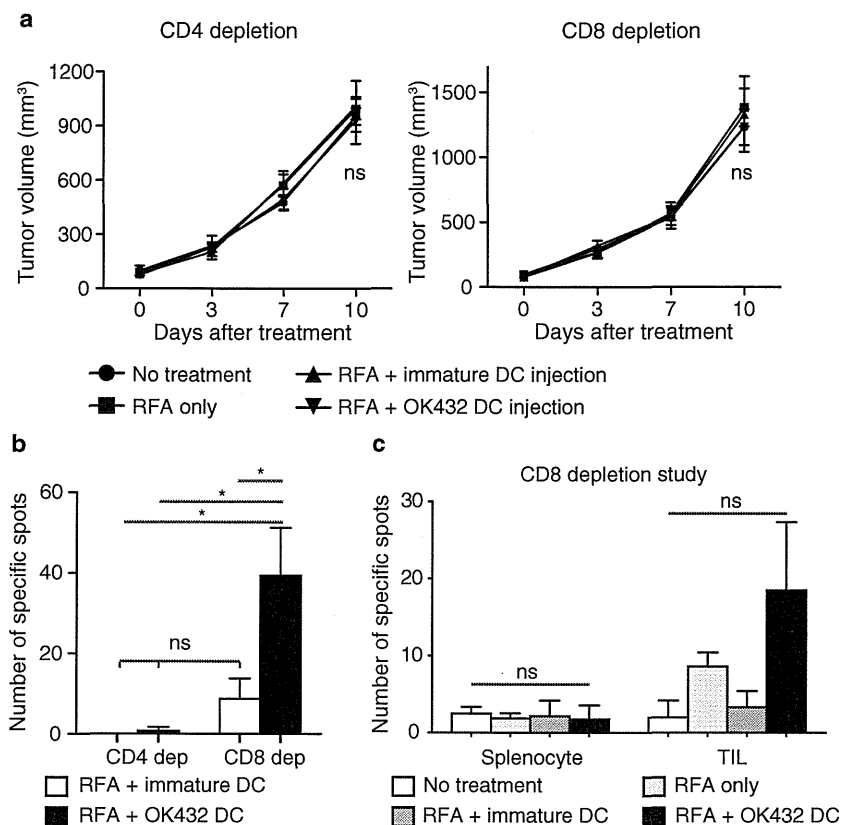


**Fig. 5** The augmented antitumor effects depended on both CD4-positive and CD8-positive cells. **a** For in vivo CD4 or CD8 depletion, monoclonal antibodies specific to CD4 (GK1.5) or CD8 (2.43), respectively, were injected intraperitoneally at 1 day before and 3 days after RFA. Tumor volumes were compared among the four groups for 10 days after RFA. In each experiment, data were obtained from four mice per group and are presented as the mean  $\pm$  SE. *ns* not significant. **b** The draining lymph nodes were harvested at 3 days

after RFA and analyzed for their tumor specificities using the IFN- $\gamma$  ELISPOT assay. Two mice were used in each group. Data are shown as the mean  $\pm$  SE. \* $P < 0.005$ ; *ns* not significant. **c** In the CD8 depletion study, splenocytes and tumor-infiltrating lymphocytes (TILs) were evaluated for their tumor specificities using the IFN- $\gamma$  ELISPOT assay as described in Fig. 3. Four mice were used in each group. Data are shown as the mean  $\pm$  SE. *ns* not significant

[32, 33]. However, in our experimental models, tumor-specific CD4-positive cells were not observed to contribute to the antitumor effect. Summarizing the above, in our study, the CD4-positive cells were required for the priming of the immune responses, and the CD8-positive cells acted as the effector cells after help from the CD4-positive cells.

In conclusion, we consider on the basis of our preclinical findings regarding combination therapy involving OK-432-stimulated DCs with RFA for the treatment of metastatic liver cancer that clinical trials can now proceed. It is anticipated that this combination therapy will be markedly superior to RFA single therapy.

**Acknowledgments** The authors thank Ms. Fushimi and Ms. Baba for technical support. This study was supported by research grants from the Ministry of Education, Culture, Sports, Science and Technology of Japan.

**Conflict of interest** The authors received financial support for this study from Chugai Pharmaceutical Co., Ltd.

## References

- Ruiterkamp J, Ernst MF, de Munck L, van der Heiden, van der Loo M, Bastiaannet E, van de Poll-Franse LV, Bosscha K, Tjan-Heijnen VC, Voogd AC (2011) Improved survival of patients with primary distant metastatic breast cancer in the period of 1995–2008. A nationwide population-based study in the Netherlands. *Breast Cancer Res Treat* 128(2):495–503. doi:10.1007/s10549-011-1349-x
- Simmonds PC, Primrose JN, Colquitt JL, Garden OJ, Poston GJ, Rees M (2006) Surgical resection of hepatic metastases from colorectal cancer: a systematic review of published studies. *Br J Cancer* 94(7):982–999. doi:10.1038/sj.bjc.6603033
- Nordlinger B, Guiguet M, Vaillant JC, Balladur P, Boudjema K, Bachellier P, Jaeck D (1996) Surgical resection of colorectal carcinoma metastases to the liver. A prognostic scoring system to improve case selection, based on 1568 patients. *Association Francaise de Chirurgie. Cancer* 77(7):1254–1262
- Bentrem DJ, Dematteo RP, Blumgart LH (2005) Surgical therapy for metastatic disease to the liver. *Annu Rev Med* 56:139–156. doi:10.1146/annurev.med.56.082103.104630
- Meyers MO, Sasson AR, Sigurdson ER (2003) Locoregional strategies for colorectal hepatic metastases. *Clin Colorectal Cancer* 3(1):34–44. doi:10.3816/CCC.2003.n.010

6. Napolitano C, Taurino F, Biffoni M, De Majo A, Coscarella G, Bellati F, Rahimi H, Pauselli S, Pellicciotta I, Burchell JM, Gaspari LA, Ercoli L, Rossi P, Rughetti A (2008) RFA strongly modulates the immune system and anti-tumor immune responses in metastatic liver patients. *Int J Oncol* 32(2):481–490
7. Nobuoka D, Motomura Y, Shirakawa H, Yoshikawa T, Kuronuma T, Takahashi M, Nakachi K, Ishii H, Furuse J, Gotohda N, Takahashi S, Nakagohri T, Konishi M, Kinoshita T, Komori H, Baba H, Fujiwara T, Nakatsura T (2012) Radiofrequency ablation for hepatocellular carcinoma induces glypican-3 peptide-specific cytotoxic T lymphocytes. *Int J Oncol* 40(1):63–70. doi:10.3892/ijo.2011.1202
8. Iida N, Nakamoto Y, Baba T, Nakagawa H, Mizukoshi E, Naito M, Mukaida N, Kaneko S (2010) Antitumor effect after radiofrequency ablation of murine hepatoma is augmented by an active variant of CC Chemokine ligand 3/macrophage inflammatory protein-1 alpha. *Cancer Res* 70(16):6556–6565. doi:10.1158/0008-5472.CAN-10-0096
9. Banchereau J, Briere F, Caux C, Davoust J, Lebecque S, Liu YJ, Pulendran B, Palucka K (2000) Immunobiology of dendritic cells. *Annu Rev Immunol* 18:767–811. doi:10.1146/annurev.immunol.18.1.767
10. Nakamoto Y, Mizukoshi E, Tsuji H, Sakai Y, Kitahara M, Arai K, Yamashita T, Yokoyama K, Mukaida N, Matsushima K, Matsui O, Kaneko S (2007) Combined therapy of transcatheter hepatic arterial embolization with intratumoral dendritic cell infusion for hepatocellular carcinoma: clinical safety. *Clin Exp Immunol* 147(2):296–305. doi:10.1111/j.1365-2249.2006.03290.x
11. Ryoma Y, Moriya Y, Okamoto M, Kanaya I, Saito M, Sato M (2004) Biological effect of OK-432 (picibanil) and possible application to dendritic cell therapy. *Anticancer Res* 24(5C):3295–3301
12. Nakahara S, Tsunoda T, Baba T, Asabe S, Tahara H (2003) Dendritic cells stimulated with a bacterial product, OK-432, efficiently induce cytotoxic T lymphocytes specific to tumor rejection peptide. *Cancer Res* 63(14):4112–4118
13. Okamoto M, Oshikawa T, Tano T, Ahmed SU, Kan S, Sasai A, Akashi S, Miyake K, Moriya Y, Ryoma Y, Saito M, Sato M (2006) Mechanism of anticancer host response induced by OK-432, a streptococcal preparation, mediated by phagocytosis and Toll-like receptor 4 signaling. *J Immunol* 29(1):78–86
14. Hovden AO, Karlsen M, Jonsson R, Appel S (2012) The bacterial preparation OK432 induces IL-12p70 secretion in human dendritic cells in a TLR3 dependent manner. *PLoS ONE* 7(2):e31217. doi:10.1371/journal.pone.0031217
15. Nakamoto Y, Mizukoshi E, Kitahara M, Arihara F, Sakai Y, Kakinoki K, Fujita Y, Marukawa Y, Arai K, Yamashita T, Mukaida N, Matsushima K, Matsui O, Kaneko S (2011) Prolonged recurrence-free survival following OK432-stimulated dendritic cell transfer into hepatocellular carcinoma during transarterial embolization. *Clin Exp Immunol* 163(2):165–177. doi:10.1111/j.1365-2249.2010.04246.x
16. Inaba K, Inaba M, Romani N, Aya H, Deguchi M, Ikehara S, Muramatsu S, Steinman RM (1992) Generation of large numbers of dendritic cells from mouse bone marrow cultures supplemented with granulocyte/macrophage colony-stimulating factor. *J Exp Med* 176(6):1693–1702
17. Mizukoshi E, Nakamoto Y, Marukawa Y, Arai K, Yamashita T, Tsuji H, Kuzushima K, Takiguchi M, Kaneko S (2006) Cytotoxic T cell responses to human telomerase reverse transcriptase in patients with hepatocellular carcinoma. *Hepatology* 43(6):1284–1294. doi:10.1002/hep.21203
18. Nakamoto Y, Suda T, Momoi T, Kaneko S (2004) Different procarcinogenic potentials of lymphocyte subsets in a transgenic mouse model of chronic hepatitis B. *Cancer Res* 64(9):3326–3333
19. Okamoto M, Furuichi S, Nishioka Y, Oshikawa T, Tano T, Ahmed SU, Takeda K, Akira S, Ryoma Y, Moriya Y, Saito M, Sone S, Sato M (2004) Expression of toll-like receptor 4 on dendritic cells is significant for anticancer effect of dendritic cell-based immunotherapy in combination with an active component of OK-432, a streptococcal preparation. *Cancer Res* 64(15):5461–5470. doi:10.1158/0008-5472.CAN-03-4005
20. Hill KS, Errington F, Steele LP, Merrick A, Morgan R, Selby PJ, Georgopoulos NT, O'Donnell DM, Melcher AA (2008) OK432-activated human dendritic cells kill tumor cells via CD40/CD40 ligand interactions. *J Immunol* 181(5):3108–3115
21. Banchereau J, Steinman RM (1998) Dendritic cells and the control of immunity. *Nature* 392(6673):245–252. doi:10.1038/32588
22. Timmerman JM, Czerwinski DK, Davis TA, Hsu FJ, Benike C, Hao ZM, Taidi B, Rajapaksa R, Caspar CB, Okada CY, van Beckhoven A, Liles TM, Engleman EG, Levy R (2002) Idiotype-pulsed dendritic cell vaccination for B-cell lymphoma: clinical and immune responses in 35 patients. *Blood* 99(5):1517–1526
23. Banchereau J, Palucka AK, Dhodapkar M, Burkeholder S, Taquet N, Rolland A, Taquet S, Coquery S, Wittkowski KM, Bhardwaj N, Pineiro L, Steinman R, Fay J (2001) Immune and clinical responses in patients with metastatic melanoma to CD34(+) progenitor-derived dendritic cell vaccine. *Cancer Res* 61(17):6451–6458
24. Okada H, Kalinski P, Ueda R, Hoji A, Kohanbash G, Donegan TE, Mintz AH, Engh JA, Bartlett DL, Brown CK, Zeh H, Holtzman MP, Reinhart TA, Whiteside TL, Butterfield LH, Hamilton RL, Potter DM, Pollack IF, Salazar AM, Lieberman FS (2011) Induction of CD8 + T-cell responses against novel glioma-associated antigen peptides and clinical activity by vaccinations with {alpha}-type I polarized dendritic cells and polyinosinic-polycytidylic acid stabilized by lysine and carboxymethylcellulose in patients with recurrent malignant glioma. *J Clin Oncol* 29(3):330–336. doi:10.1200/JCO.2010.30.7744
25. Suso EM, Dueland S, Rasmussen AM, Vethrus T, Aamdal S, Kvalheim G, Gaudernack G (2011) hTERT mRNA dendritic cell vaccination: complete response in a pancreatic cancer patient associated with response against several hTERT epitopes. *Cancer Immunol Immunother* 60(6):809–818. doi:10.1007/s00262-011-0991-9
26. Frey B, Weiss EM, Rubner Y, Wunderlich R, Ott OJ, Sauer R, Fietkau R, Gaipl US (2012) Old and new facts about hyperthermia-induced modulations of the immune system. *Int J Hyperthermia* 28(6):528–542. doi:10.3109/02656736.2012.677933
27. Rubner Y, Wunderlich R, Ruhle PF, Kulzer L, Werthmoller N, Frey B, Weiss EM, Keilholz L, Fietkau R, Gaipl US (2012) How does ionizing irradiation contribute to the induction of anti-tumor immunity? *Front Oncol* 2:75. doi:10.3389/fonc.2012.00075
28. den Brok MH, Suttmuller RP, van der Voort R, Bennink EJ, Figdor CG, Ruers TJ, Adema GJ (2004) In situ tumor ablation creates an antigen source for the generation of antitumor immunity. *Cancer Res* 64(11):4024–4029. doi:10.1158/0008-5472.CAN-03-3949
29. Forster R, Schubel A, Breitfeld D, Kremmer E, Renner-Muller I, Wolf E, Lipp M (1999) CCR7 coordinates the primary immune response by establishing functional microenvironments in secondary lymphoid organs. *Cell* 99(1):23–33
30. Ferlazzo G, Tsang ML, Moretta L, Melioli G, Steinman RM, Munz C (2002) Human dendritic cells activate resting natural killer (NK) cells and are recognized via the NKp30 receptor by activated NK cells. *J Exp Med* 195(3):343–351
31. Morandi B, Mortara L, Chiassone L, Accolla RS, Mingari MC, Moretta L, Moretta A, Ferlazzo G (2012) Dendritic cell editing by activated natural killer cells results in a more protective cancer-specific immune response. *PLoS ONE* 7(6):e39170. doi:10.1371/journal.pone.0039170